microscope (Olympus, Tokyo, Japan) or an All-in-One BZ-9000 Fluorescence microscope (KEYENCE, Osaka, Japan). Digital image Z-stacks were created, and projections were made from them using an Olympus FV1000 microscope and FV10-ASW software (Olympus). Fluorescence intensity was measured using the NIH Image J Program.

2.5. Quantification of cellular Purkinje cell size

Sixteen-micrometer stacks of cerebellar optical sections were collected using an All-in-One BZ-9000 Fluorescence microscope and Z-stack images were joined into sagittal images using BZ-II software (KEYENCE). These data were transferred into Neurolucida software (MBF Bioscience, Japan, Inc., Chiba, Japan). Four stacks (each 0.09 μm^2 in area) for each of three sections from WT, HGF-Tg, SCA7-KI, and SCA7-KI/HGF-Tg mice ($n=3$ each) were used to measure the cell sizes of calbindin-positive Purkinje cells. Quantification of cell size was performed as previously described with slight modifications (Yoo et al., 2003). Briefly, each cell surface was outlined manually. The perikaryon area of each cell was estimated to be the approximately circular area enclosed by the cell perimeter and the extension of the cell perimeter toward the initial point of dendrite extension. Partial cells and binary cell images were excluded based upon cell shape and relative fluorescence intensity.

2.6. Enzyme-linked immunosorbent assay (ELISA)

After the mice were placed under deep anesthesia with an overdose of sodium pentobarbital, the cerebella of WT, HGF-Tg, SCA7-KI, and SCA7-KI/HGF-Tg mice ($n=4$ each) were collected, quickly frozen and stored at −80 °C until used. Frozen tissue samples were homogenized, subsequently sonicated using a Bioruptor UCD-250 (Cosmo Bio Co., Ltd., Tokyo, Japan), and centrifuged at 4 °C. The supernatants were then used to quantify HGF protein levels using ELISA (Institute of Immunology Co., Ltd., Tokyo, Japan) as previously described (Kadoyama et al., 2007; Sun et al., 2002; Yamada et al., 1995).

2.7. Assessment of motor performance

A rotarod apparatus (Bioseb, Paris, France) was used to assess the ability of an animal to balance on an elevating rotating metal rod (Carter et al., 2001). Rotarod tests are a common tool of studies of mouse models of spinocerebellar ataxia (Yoo et al., 2003; Custer et al., 2006). In this study, 10-week-old mice (WT; $n=13$, HGF-Tg; $n=12$, SCA7-KI; $n=12$, SCA7-KI/HGF-Tg; $n=8$) were placed on the rotarod, the speed of which was set at 5 rpm initially and accelerated until reaching a speed of 20 rpm for 5 min. After taking a rest for more than 5 min, the latency to fall from the rotarod was measured for 5 min using the machine mode (initial rate of 5 rpm; acceleration until reaching 40 rpm for 10 min). The average latency to fall for each genotype was calculated.

2.8. Statistical analyses

Statistical analyses were carried out using StatView software version 5.0.1 (SAS institute, Cary, NC). Differences in the total intensities of immunostaining for HGF, GLAST, GLT1, size of Purkinje cells, and regional HGF levels in the cerebellum among the above animal models were all determined by one-way ANOVA with Fisher's PLSD tests. Latency to fall in rotarod tests was analyzed using the Student's t-test. The results are presented as the mean ± S.E.M. A value of $P<0.05$ was considered statistically significant.

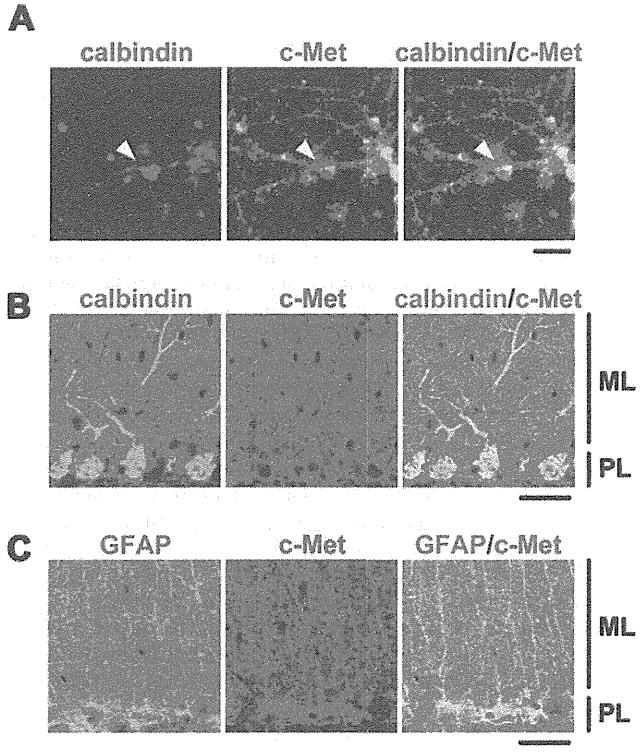

Fig. 1. Immunocytochemical and immunohistochemical localization of c-Met in cerebellar cells *in vitro* and *in vivo*. HGF receptor (c-Met) is expressed in Purkinje cells of the mouse cerebellum *in vitro* and *in vivo*. (A) Immunocytochemistry in primary neuronal cultures of the cerebellum from E16 mouse embryos. Purkinje cells show double immunoreactivity (white arrowheads) for calbindin (red) and c-Met (green) in culture. Bar, 30 μm. (B and C) Immunohistochemistry in 10-week-old wild-type (WT) mice. (B) Purkinje cells show double immunoreactivity against calbindin (green) and c-Met (red). PL, Purkinje cell layer; ML, molecular layer. Bar, 30 μm. (C) Bergmann glia show double immunoreactivity against GFAP (green) and c-Met (red). Bar, 30 μm. (For interpretation of the references to color in this figure caption, the reader is referred to the web version of the article.) Q3

3. Results

3.1. c-Met is expressed in the cerebellar Purkinje cells in vitro

To assess whether cerebellar Purkinje cells are potential target cells of HGF, we first performed double immunostaining of c-Met (green) and calbindin (red), a marker for Purkinje cells, in primary cultures of embryonic mouse cerebellar neurons *in vitro*. c-Met-immunoreactivity (IR) was observed in a large number of cerebellar neurons, with most of these presumably being granular cells. In addition to these neurons, c-Met-IR was indeed detected in calbindin-positive Purkinje cells (Fig. 1A).

3.2. c-Met is expressed in the cerebellar Purkinje cells and Bergmann glia in vivo

We next assessed whether c-Met is expressed in Purkinje cells *in vivo* using double immunostaining for c-Met (red) and calbindin (green) in the cerebella of WT mice. c-Met-IR was detected in Purkinje cells of the cerebella of WT mice. In addition, c-Met-IR was detected in other cells surrounding to the Purkinje cells (Fig. 1B). These cells that were closely apposed to Purkinje cells resembled Bergmann glia. To determine if these non-Purkinje cells were Bergmann glia, double immunostaining for c-Met (red) and GFAP (green), a marker for Bergmann glia, was performed. As shown in Fig. 1C, c-Met-IR was detected in Bergmann glia. These findings

Please cite this article in press as: Noma, S., et al., Overexpression of HGF attenuates the degeneration of Purkinje cells and Bergmann glia in a knockin mouse model of spinocerebellar ataxia type 7. Neurosci. Res. (2012), doi:10.1016/j.neures.2012.03.001

indicate that both Purkinje cells and Bergmann glia are potential target cells of HGF *in vivo*.

3.3. Immunohistochemical analyses of HGF and phospho-c-Met in the cerebellum of WT, HGF-Tg, SCA7-KI, and SCA7-KI/HGF-Tg mice

To explore whether HGF can modify the degeneration of Purkinje cells in SCA7-KI mice, we used neuron-specific enolase (NSE)-driven HGF overexpression transgenic mice (HGF-Tg) to introduce HGF into the Purkinje cells of SCA7-KI mice. Crossing SCA7-KI mice with HGF-Tg mice generated the following four mouse models: (1) wild-type littermates (WT), (2) HGF-Tg, (3) SCA7-KI, and (4) SCA7-KI/HGF-Tg mice. This approach allowed the stable introduction of the HGF gene directly into the cerebellar neurons of SCA7-KI mice. Confirmation that HGF was introduced into the cerebellum of SCA7-KI/HGF-Tg mice was accomplished with immunostaining. HGF-IR was faintly detected in calbindin-positive Purkinje cells and GFAP-positive Bergman glia of the cerebellum in WT and SCA7-KI mice (Fig. 2A, upper panel), while more intense staining of HGF-IR was detected in Purkinje cells of HGF-Tg mice as well as in SCA7-KI/HGF-Tg mice (Fig. 2A, bottom panel). In addition to Purkinje cells, HGF-IR was detected in cells surrounding the Purkinje cells, *i.e.* GFAP-positive Bergmann glia. These findings were further confirmed by quantitative analyses of the immunofluorescent intensity of HGF-IR in sections of the cerebellum (Fig. 2B) and HGF content using ELISA analyses (Fig. 2C). These findings suggest that overexpressed HGF in cerebellar neurons is released into the extracellular space, and is in turn distributed to Bergmann glia.

3.4. c-Met is tyrosine-phosphorylated in Purkinje cells and Bergmann glia in SCA7-KI/HGF-Tg mice

Further attempts were made to determine if overexpression of HGF contributes to tyrosine-phosphorylation, and thereby activation, of c-Met in SCA7-KI/HGF-Tg mice. The level of phospho-c-Met-IR was much higher in both the Purkinje cells and Bergmann glia of SCA7-KI/HGF-Tg mice compared to those of SCA7-KI mice. These findings demonstrate that overexpression of HGF in SCA7-KI/HGF-Tg mice contributes to the activation of c-Met in Purkinje cells and Bergmann glia, prompting an examination of the role of HGF in the modulation of these cells in SCA7-KI mice (Fig. 2D).

3.5. Overexpression of HGF attenuates the degeneration of Purkinje cells of the cerebellum in SCA7-KI mice

To elucidate whether HGF plays a role in attenuating the degeneration of Purkinje cells in SCA7-KI mice, we next compared the morphology of Purkinje cells from the cerebella of SCA7-KI and SCA7-KI/HGF-Tg mice. Calbindin immunohistochemistry revealed that Purkinje cells appeared to have large spherical cell bodies in both WT and HGF-Tg mice, while a number of Purkinje cells with reduced cellular size (degenerated neurons, white arrowheads), were present in SCA7-KI mice (Fig. 3A). In contrast, many more large spherical neurons were observed in SCA7-KI/HGF-Tg mice compared to SCA7-KI mice (Fig. 3A). The size distribution of Purkinje cells in WT, HGF-Tg, SCA7-KI, and SCA7-KI/HGF-Tg mice is shown in Fig. 3B. Quantitative analyses showed that the size of Purkinje cells in SCA7-KI mice was varied from small (<150 μm^2) to large (>150 μm^2; healthy), while the quantity of small Purkinje cells (<150 μm^2) was reduced in SCA7-KI/HGF-Tg mice (Fig. 3B). Namely, the fraction of small Purkinje cells was significantly lower in SCA7-KI/HGF-Tg mice than in SCA7-KI mice. These findings demonstrate that overexpression of HGF attenuates the degeneration of Purkinje cells in SCA7-KI mice.

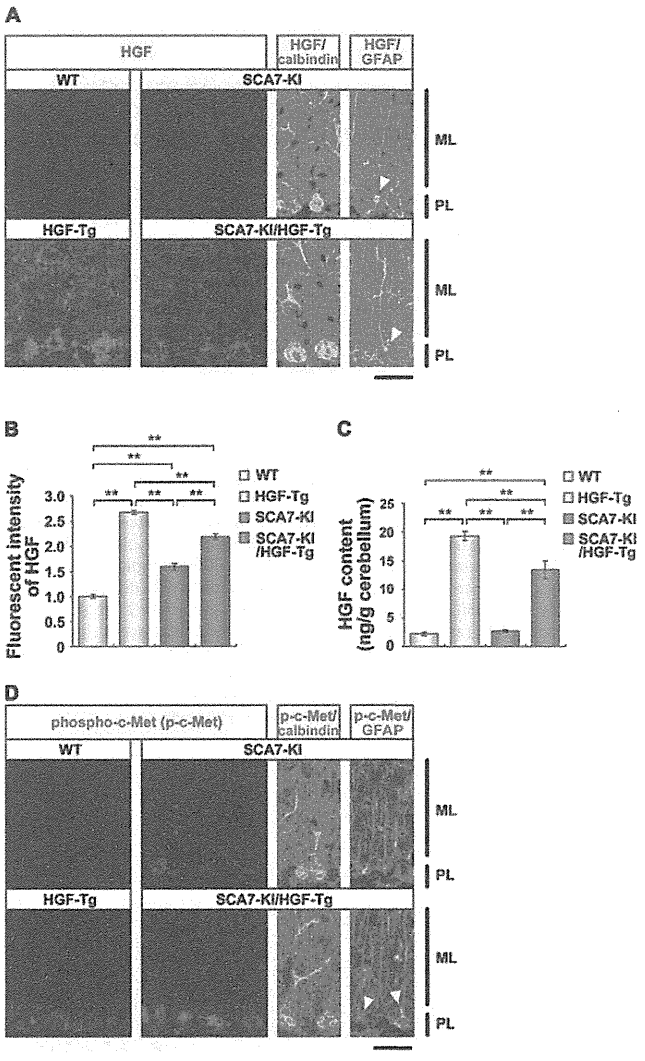

Fig. 2. Immunohistochemical localization of HGF and phospho-c-Met in cerebellar cells *in vivo*. Comparison of HGF levels by immunohistochemistry (A and B) and HGF ELISA (C) in the cerebellum of 10-week-old WT, HGF-Tg, SCA7-KI, and SCA7-KI/HGF-Tg mice using anti-rat HGF that detects both endogenous and exogenous (overexpressed) HGF proteins. (A) HGF-IR is elevated in HGF-Tg and SCA7-KI/HGF-Tg mice. PL, Purkinje cell layer; ML, molecular layer. Bar, 30 μm. White arrowhead indicates GFAP/HGF double-positive cells. (B) Fluorescent intensity ($n = 6$ per group) of HGF in each group. Mean HGF signal intensity was significantly elevated compared to WT (**$P < 0.01$, Fisher's PLSD test). Error bars indicate S.E.M. (C) HGF protein levels in the whole cerebellum are elevated in HGF-Tg and SCA7-KI/HGF-Tg mice ($n = 4$ per group, **$P < 0.01$, Fisher's PLSD test). Error bars indicate S.E.M. (D) Immunohistochemistry of tyrosine phosphorylation at positions 1230, 1234, and 1235 of c-Met (phospho-c-Met, red) in the cerebellum in 10-week-old mice. Phospho-c-Met staining is shown in the cerebellum in all mice groups. Phospho-c-Met-IR is elevated in both Purkinje cells (lower left panel, green) and Bergmann glia (lower right panel, green) of SCA7-KI/HGF-Tg mice compared to SCA7-KI mice (upper panel, green). White arrowheads indicate GFAP/phospho-c-Met double-positive cells. Bar, 30 μm. (For interpretation of the references to color in this figure caption, the reader is referred to the web version of the article.)

3.6. Overexpression of HGF maintains the levels of the glutamate transporters (GLAST and GLT-1) in the cerebellum of SCA7-KI mice

Bergmann glia are responsible for glutamate uptake (removal) from the Purkinje cell synaptic cleft. It has been suggested that polyglutamine-expanded ataxin-7 induces Purkinje cell excitotoxicity by interfering with Bergmann glia-mediated glutamate uptake. This is due to the fact that the expression of GLAST, a

Please cite this article in press as: Noma, S., et al., Overexpression of HGF attenuates the degeneration of Purkinje cells and Bergmann glia in a knockin mouse model of spinocerebellar ataxia type 7. Neurosci. Res. (2012), doi:10.1016/j.neures.2012.03.001

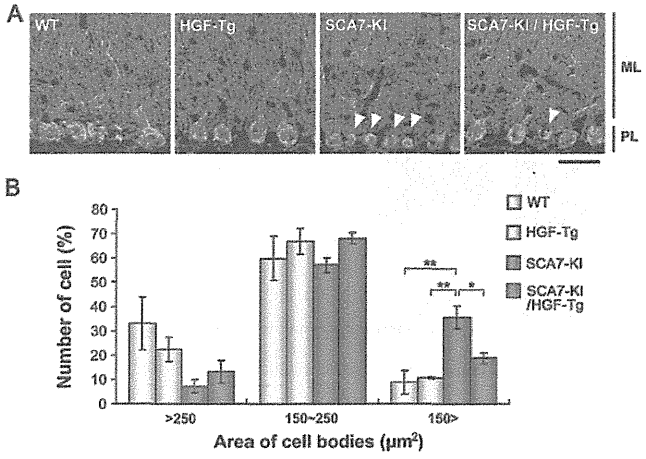

Fig. 3. HGF attenuates degeneration of Purkinje cell bodies. (A) Immunohistochemistry of calbindin (green) in the cerebellum of 10-week-old mice. SCA7-KI mice displayed smaller Purkinje cell body size than WT and HGF-Tg mice. SCA7-KI/HGF-Tg mice showed an attenuation of shrinkage of Purkinje cell bodies. PL, Purkinje cell layer; ML, molecular layer. Bar, 30 μm. White arrowhead indicates degenerative Purkinje cell changes. (B) Quantification of cell numbers with different Purkinje cellular body size (>250; 150–250; <150 μm^2) of each group ($n = 3$ per group). The number of small cells (area are less than 150 μm^2) in SCA7-KI mice is significantly greater *versus* WT and HGF-Tg mice (**$P < 0.01$, Fisher's PLSD test), SCA7-KI/HGF-Tg mice exhibit significantly fewer small cells compared to SCA7-KI mice (*$P < 0.05$). Error bars indicate S.E.M. (For interpretation of the references to color in this figure caption, the reader is referred to the web version of the article.)

glutamate transporter in the cerebellum, is confined to Bergmann glia and marked reductions in GLAST expression (and glutamate uptake) have been observed in presymptomatic Gfa2-SCA7-92Q mice (Custer et al., 2006). As c-Met is expressed in the Bergmann glia of WT mice and is phosphorylated (*i.e.* activated) in Bergmann glia in SCA7-KI/HGF-Tg mice (Figs. 1C and 2D), we next examined whether HGF affects the morphology and function of Bergmann glia. Immunostaining for GFAP revealed that obvious morphological difference of Bergmann glia was not detected between WT mice and SCA7-KI/HGF-Tg mice (Fig. 4A). We then examined whether HGF modulates the down-regulation of GLAST levels in SCA7-KI mice. Immunostaining for GLAST revealed that GLAST levels were decreased in SCA7-KI mice compared to WT mice, while the levels were generally maintained in SCA7-KI/HGF-Tg mice (Fig. 4B and C). These findings demonstrate that HGF supports GLAST levels in SCA7-KI mice. We then examined HGF regulation of GLT-1, another glutamate transporter that is also abundant in the cerebellum, by a similar mechanism. Immunostaining for GLT-1 revealed that the levels of GLT-1 were markedly decreased in SCA7-KI mice compared to WT mice, while the level was maintained or even increased in SCA7-KI/HGF-Tg mice (Fig. 4D and E). These findings demonstrate that HGF maintains or even increases the levels of GLT-1 in SCA7-KI mice.

3.7. *Overexpression of HGF improves rotarod performance in SCA7-KI mice*

Data obtained so far suggested that SCA7 could be improved by HGF *via* the attenuation of Purkinje cellular degeneration and reduction of glutamate transporters in Bergmann glia. Therefore, we examined whether these improvements were reflected by

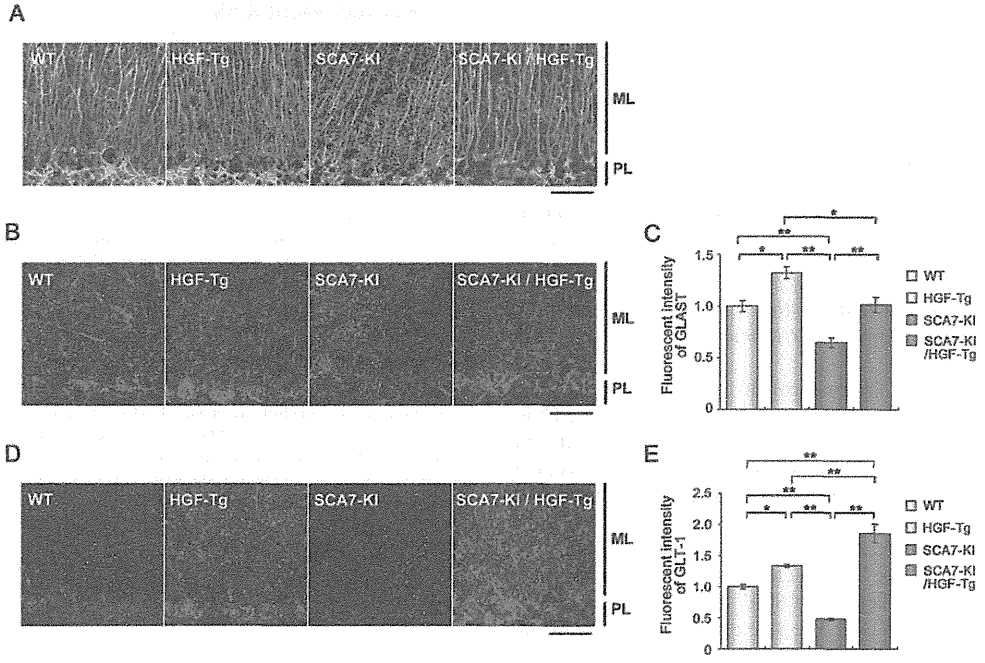

Fig. 4. HGF maintains the levels of glutamate transporters (GLAST and GLT-1) in Bergmann glia in the cerebellum of SCA7-KI mice. (A) Immunohistochemistry for Bergmann glia (GFAP, green) in the cerebellum in 10-week-old mice. No significant alterations were detected in the morphology of Bergmann glia. PL, Purkinje cell layer; ML, molecular layer. Bar, 30 μm. (B and C) Comparison of GLAST levels in 10-week-old mice. (B) Immunohistochemistry for GLAST in the cerebellum. GLAST staining is reduced in the SCA7-KI mouse cerebellum and is significantly rescued in the SCA7-KI/HGF-Tg cerebellum. Bar, 30 μm. (C) Quantification of fluorescent intensity ($n = 3$ per group) of PL. Mean GLAST signal intensity is significantly elevated in SCA7-KI/HGF-Tg cerebellum *versus* SCA7-KI cerebellum (*$P < 0.05$, **$P < 0.01$, Fisher's PLSD test). Error bars indicate S.E.M. (D and E) Comparison of GLT-1 level at 10-week-old mice. (D) Immunohistochemistry for GLT-1 in the cerebellum. GLT-1 staining is reduced in the cerebellum of SCA7-KI mice, while significantly elevated in the cerebellum of SCA7-KI/HGF-Tg mice. Bar, 30 μm. (E) Mean fluorescent intensity ($n = 3$ per group) of PL. Mean GLT-1 signal intensity is significantly elevated in the cerebellum of SCA7-KI/HGF-Tg mice (*$P < 0.05$, **$P < 0.01$, Fisher's PLSD test). Error bars indicate S.E.M. (For interpretation of the references to color in this figure caption, the reader is referred to the web version of the article.)

Please cite this article in press as: Noma, S., et al., Overexpression of HGF attenuates the degeneration of Purkinje cells and Bergmann glia in a knockin mouse model of spinocerebellar ataxia type 7. Neurosci. Res. (2012), doi:10.1016/j.neures.2012.03.001

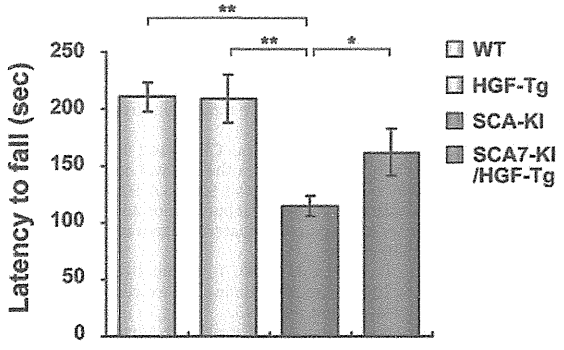

Fig. 5. HGF improves coordinated motor behavior of SCA7-KI mice. Comparison of motor coordination in 10-week-old WT, HGF-Tg, SCA7-KI, and SCA7-KI/HGF-Tg mice using the rotarod test. SCA7-KI/HGF-Tg mice display improved rotarod performance compared to SCA7-KI mice ($n = 8–12$ per group; $^{*}P < 0.05$, $^{**}P < 0.01$, Student's t test). Error bars indicate S.E.M.

motor performance of WT, HGF-Tg, SCA7-KI, and SCA7-KI/HGF-Tg mice. To examine the ability of an animal to balance on a rotating rod, rotarod tests were applied on each animal at 10 weeks of age. There was a marked reduction in the latency to fall in SCA7-KI mice compared to WT and HGF-Tg mice. However, the latency to fall of SCA7-KI/HGF-Tg mice was significantly longer than that of SCA7-KI mice (Fig. 5), suggesting that overexpression of HGF contributes to the amelioration of rotarod performance impairments in SCA7-KI mice.

4. Discussion

In the present study, we examined whether overexpression of HGF, a pleiotrophic growth factor with highly potent neurotrophic activities, exhibits a beneficial function in SCA7-KI mice. By crossing SCA7-KI mice with HGF-Tg mice that overexpress HGF under the NSE promoter, four groups of mice (WT, HGF-Tg, SCA7-KI, and SCA7-KI/HGF-Tg mice) were generated. The results indicate that overexpression of HGF attenuates the degeneration of Purkinje cells, maintains the levels of the glutamate transporters GLAST and GLT-1 in Bergmann glia and improves rotarod performance deficits observed in SCA7-KI mice.

The molecular mechanisms responsible for these events have not yet been clarified in detail. However, because HGF protein is expressed and distributed in Purkinje cells and Bergmann glia in SCA7-KI/HGF-Tg mice at much higher levels than in SCA7-KI mice, and because the expression and phosphorylation (activation) of c-Met was observed at much higher levels in both the Purkinje cells and Bergmann glia of SCA7-KI/HGF-Tg mice, it seems likely that HGF functions directly on Purkinje cells as well as Bergmann glia. If there is a direct interaction, the ability of HGF to function not only on Purkinje cells but also on Bergmann glia might represent a therapeutic opportunity for attenuating the degeneration of Purkinje cells, since recent genetic approaches suggest that an important mutual interaction of Purkinje cells and Bergmann glia in SCA7 might, at least in part, be involved in the degeneration of these cells in this disease (Custer et al., 2006; Furrer et al., 2011). Furthermore, Bergmann glia are also shown to secrete neurotrophic factors that support Purkinje cells (Mount et al., 1995).

Purkinje cells are integrated into a complex neural network and receive glutamatergic input from axons projecting from the inferior olive and cerebellar granule cells. Hence, in addition to Purkinje cells and Bergmann glia, which we focused on the present study, other cells and their neural networks in the cerebellum may also play a role in the pathogenesis of disease models of SCA7 and related diseases (Gatchel et al., 2007; Furrer et al., 2011). For example, transcriptional down-regulation of insulin-like growth factor binding protein 5 (*igfbp5*) in cerebellar granule cells is proposed to be involved in non-cell-autonomous degeneration of Purkinje cells in SCA7-KI mice (Gatchel et al., 2007). It has not yet been determined whether HGF could alleviate reduction of *igfbp5*, and this possibility is worth examining in a future study. Given that HGF elicits neurotrophic activity on cerebellar granular cells both *in vitro* and *in vivo* (Zhang et al., 2000; Ieraci et al., 2002), we cannot exclude the possibility that HGF functions on granular cells and alleviates the down-regulation of *igfbp5*. Therefore, HGF may also contribute to attenuation of Purkinje cell degeneration *via* cerebellar granular cells.

It has not yet been determined whether HGF alleviates the degeneration of the retina, the other region associated with phenotypic changes appearing in SCA7-KI mice. HGF and c-Met are expressed in various populations of rat retinal neurons during development as well as in the adult, and neuroprotective effects of HGF on rat retinal photoreceptors have been reported (Machida et al., 2004; Ohtaka et al., 2006; Shibuki et al., 2002; Sun et al., 1999).

The rotarod test is used to analyze motor phenotype, in the aspect of motor balance and/or its coordination (Carter et al., 2001; Custer et al., 2006). Hence, the ability of HGF to improve rotarod performance raises the potential utility of HGF for the improvement of motor impairment of affected individuals. However, further experiments are required to address the relationship between the outcome of rotarod tests in the present study and the clinical ataxic phenotype of SCA7.

Cvetanovic et al. (2011) recently reported that genetic overexpression or pharmacologic infusion of recombinant vascular endothelial growth factor (VEGF) ameliorates the ataxic phenotype and degeneration of Purkinje cells in a mouse model of another type of spinocerebellar ataxia, spinocerebellar ataxia type 1 (SCA1). Given that HGF promotes angiogenesis in a variety of disease models (Funakoshi and Nakamura, 2003, 2011) and that c-Met is not only expressed in Purkinje cells and Bergmann glia but also in other types of cells including vascular cells and neural progenitor populations in WT mice (Funakoshi and Nakamura, 2011; Noma et al., unpublished results), it would be interesting to know how HGF plays a role in SCA1-model mice and whether HGF promotes angiogenesis and neurogenesis in SCA7-KI mice. It should be noted that exercise produces beneficial effects in alleviating SCA1 symptoms in mice (Fryer et al., 2011). Exercise is known to promote HGF production in some patients (Yasuda et al., 2004) and that HGF improves the phenotype of SCA7-KI as shown in the present study. Hence, it would also be interesting to examine whether exercise plays a role in the attenuation of the progression of the course of SCA7-KI pathology and if HGF is involved in the process.

In summary, the present study provided the first evidence that overexpression of HGF is beneficial for attenuating the degeneration of both Purkinje cells and Bergmann glia. Considered with the notion that intrathecal injection of recombinant human HGF protein has been shown to be effective in several disease models, such as a transgenic rat model of ALS (Ishigaki et al., 2007) and a primate model of spinal cord injury (Kitamura et al., 2011), our findings may raise the possibility of a therapeutic use of HGF in SCA7 and related disorders.

Acknowledgements

This work was supported in part by Grants-in-Aid from the Ministry of Health, Labour and Welfare of Japan and Grants-in-Aid from the Ministry of Education, Science, and Culture of Japan. We wish to thank Prof. Huda Y. Zoghbi for providing us the SCA7-KI mice. We are grateful to Ms. Higano, Ms. Ikushima and Ms. Yoneda for secretarial assistance.

Please cite this article in press as: Noma, S., et al., Overexpression of HGF attenuates the degeneration of Purkinje cells and Bergmann glia in a knockin mouse model of spinocerebellar ataxia type 7. Neurosci. Res. (2012), doi:10.1016/j.neures.2012.03.001

References

Carter, R.J., Morton, J., Dunnett, S.B., 2001. Motor coordination and balance in rodents. Curr. Protoc. Neurosci. (Chapter 8): Unit 8.12.
Custer, S.K., Garden, G.A., Gill, N., Rueb, U., Libby, R.T., Schultz, C., Guyenet, S.J., Deller, T., Westrum, L.E., Sopher, B.L., La Spada, A.R., 2006. Bergmann glia expression of polyglutamine-expanded ataxin-7 produces neurodegeneration by impairing glutamate transport. Nat. Neurosci. 9, 1302–1311.
Cvetanovic, M., Patel, J.M., Marti, H.H., Kini, A.R., Opal, P., 2011. Vascular endothelial growth factor ameliorates the ataxic phenotype in a mouse model of spinocerebellar ataxia type 1. Nat. Med. 17, 1445–1447.
Fryer, J.D., Yu, P., Kang, H., Mandel-Brehm, C., Carter, A.N., Crespo-Barreto, J., Gao, Y., Flora, A., Shaw, C., Orr, H.T., Zoghbi, H.Y., 2011. Exercise and genetic rescue of SCA1 via the transcriptional repressor Capicua. Science 334, 690–693.
Funakoshi, H., Nakamura, T., 2003. Hepatocyte growth factor: from diagnosis to clinical applications. Clin. Chim. Acta 327, 1–23.
Funakoshi, H., Nakamura, T., 2011. Hepatocyte growth factor (HGF): neurotrophic functions and therapeutic implications for neuronal injury/diseases. Curr. Signal Transduct. Ther. 6, 156–167.
Furrer, S.A., Mohanachandran, M.S., Waldherr, S.M., Chang, C., Damian, V.A., Sopher, B.L., Garden, G.A., La Spada, A.R., 2011. Spinocerebellar ataxia type 7 cerebellar disease requires the coordinated action of mutant ataxin-7 in neurons and glia, and displays non-cell-autonomous Bergmann glia degeneration. J. Neurosci. 31, 16269–16278.
Huang, H., Bordey, A., 2004. Glial glutamate transporters limit spillover activation of presynaptic NMDA receptors and influence synaptic inhibition of Purkinje neurons. J. Neurosci. 24, 5659–5669.
Honda, S., Kagoshima, M., Wanaka, A., Tohyama, M., Matsumoto, K., Nakamura, T., 1995. Localization and functional coupling of HGF and c-Met/HGF receptor in rat brain: implication as neurotrophic factor. Brain Res. Mol. Brain Res. 32, 197–210.
Hossain, M.A., Russell, J.C., Gomez, R., Laterra, J., 2002. Neuroprotection by scatter factor/hepatocyte growth factor and FGF-1 in cerebellar granule neurons is phosphatidylinositol 3-kinase/akt-dependent and MAPK/CREB-independent. J. Neurochem. 81, 365–378.
Ieraci, A., Forni, P.E., Ponzetto, C., 2002. Viable hypomorphic signaling mutant of the Met receptor reveals a role for hepatocyte growth factor in postnatal cerebellar development. Proc. Natl. Acad. Sci. U.S.A. 99, 15200–15205.
Ishigaki, A., Aoki, M., Nagai, M., Warita, H., Kato, S., Kato, M., Nakamura, T., Funakoshi, H., Itoyama, Y., 2007. Intrathecal delivery of hepatocyte growth factor from amyotrophic lateral sclerosis onset suppresses disease progression in rat amyotrophic lateral sclerosis model. J. Neuropathol. Exp. Neurol. 66, 1037–1044.
Kadoyama, K., Funakoshi, H., Ohya, W., Nakamura, T., 2007. Hepatocyte growth factor (HGF) attenuates gliosis and motoneuronal degeneration in the brainstem motor nuclei of a transgenic mouse model of ALS. Neurosci. Res. 59, 446–456.
Kitamura, K., Fujiyoshi, K., Yamane, J., Toyota, F., Hikishima, K., Nomura, T., Funakoshi, H., Nakamura, T., Aoki, M., Toyama, Y., Okano, H., Nakamura, M., 2011. Human hepatocyte growth factor promotes functional recovery in primates after spinal cord injury. PLoS One 6, e27706.
Machida, S., Tanaka, M., Ishii, T., Ohtaka, K., Takahashi, T., Tazawa, Y., 2004. Neuroprotective effect of hepatocyte growth factor against photoreceptor degeneration in rats. Invest. Ophthalmol. Vis. Sci. 45, 4174–4182.
Miyazawa, T., Matsumoto, K., Ohmichi, H., Katoh, H., Yamashima, T., Nakamura, T., 1998. Protection of hippocampal neurons from ischemia-induced delayed neuronal death by hepatocyte growth factor: a novel neurotrophic factor. J. Cereb. Blood Flow Metab. 18, 345–348.
Mount, H.T., Dean, D.O., Alberch, J., Dreyfus, C.F., Black, I.B., 1995. Glial cell line-derived neurotrophic factor promotes the survival and morphologic differentiation of Purkinje cells. Proc. Natl. Acad. Sci. U.S.A. 92, 9092–9096.
Nakamura, T., Nawa, K., Ichihara, A., 1984. Partial purification and characterization of hepatocyte growth factor from serum of hepatectomized rats. Biochem. Biophys. Res. Commun. 122, 1450–1459.
Nakamura, T., Nishizawa, T., Hagiya, M., Seki, T., Shimonishi, M., Sugimura, A., Tashiro, K., Shimizu, S., 1989. Molecular cloning and expression of human hepatocyte growth factor. Nature 342, 440–443.
Ohtaka, K., Machida, S., Ohzeki, T., Tanaka, M., Kurosaka, D., Masuda, T., Ishii, T., 2006. Protective effect of hepatocyte growth factor against degeneration of the retinal pigment epithelium and photoreceptor in sodium iodate-injected rats. Curr. Eye Res. 31, 347–355.
Ohya, W., Funakoshi, H., Kurosawa, T., Nakamura, T., 2007. Hepatocyte growth factor (HGF) promotes oligodendrocyte progenitor cell proliferation and inhibits its differentiation during postnatal development in the rat. Brain Res. 1147, 51–65.
Shibuki, H., Katai, N., Kuroiwa, S., Kurokawa, T., Arai, J., Matsumoto, K., Nakamura, T., Yoshimura, N., 2002. Expression and neuroprotective effect of hepatocyte growth factor in retinal ischemia-reperfusion injury. Invest. Ophthalmol. Vis. Sci. 43, 528–536.
Sun, W., Funakoshi, H., Nakamura, T., 1999. Differential expression of hepatocyte growth factor and its receptor, c-Met in the rat retina during development. Brain Res. 851, 46–53.
Sun, W., Funakoshi, H., Nakamura, T., 2002. Overexpression of HGF retards disease progression and prolongs life span in a transgenic mouse model of ALS. J. Neurosci. 22, 6537–6548.
Yamada, A., Matsumoto, K., Iwanari, H., Sekiguchi, K., Kawata, S., Matsuzawa, Y., Nakamura, T., 1995. Rapid and sensitive enzyme-linked immunosorbent assay for measurement of HGF in rat and human tissues. Biomed. Res. 16, 105–114.
Yasuda, S., Goto, Y., Takaki, H., Asaumi, Y., Baba, T., Miyazaki, S., Nonogi, H., 2004. Exercise-induced hepatocyte growth factor production in patients after acute myocardial infarction: its relationship to exercise capacity and brain natriuretic peptide levels. Circ. J. 68, 304–307.
Yoo, S.Y., Pennesi, M.E., Weeber, E.J., Xu, B., Atkinson, R., Chen, S., Armstrong, D.L., Wu, S.M., Sweatt, J.D., Zoghbi, H.Y., 2003. SCA7 knockin mice model human SCA7 and reveal gradual accumulation of mutant ataxin-7 in neurons and abnormalities in short-term plasticity. Neuron 37, 383–401.
Zhang, L., Himi, T., Morita, I., Murota, S., 2000. Hepatocyte growth factor protects cultured rat cerebellar granule neurons from apoptosis via the phosphatidylinositol-3 kinase/Akt pathway. J. Neurosci. Res. 59, 489–496.

Please cite this article in press as: Noma, S., et al., Overexpression of HGF attenuates the degeneration of Purkinje cells and Bergmann glia in a knockin mouse model of spinocerebellar ataxia type 7. Neurosci. Res. (2012), doi:10.1016/j.neures.2012.03.001

SAGE-Hindawi Access to Research
Leukemia Research and Treatment
Volume 2011, Article ID 726964, 11 pages
doi:10.4061/2011/726964

Review Article

Characterization of Kaposi's Sarcoma-Associated Herpesvirus-Related Lymphomas by DNA Microarray Analysis

Keiji Ueda, Eriko Ohsaki, Kazushi Nakano, and Xin Zheng

Division of Virology, Department of Microbiology and Immunology, Osaka University Graduate School of Medicine, 2-2 Yamada-oka, Suita, Osaka 565-0871, Japan

Correspondence should be addressed to Keiji Ueda, kueda@virus.med.osaka-u.ac.jp

Received 26 June 2011; Accepted 2 September 2011

Academic Editor: Daniela Cilloni

Among herpesviruses, γ-herpesviruses are supposed to have typical oncogenic activities. Two human γ-herpesviruses, Epstein-Barr virus (EBV) and Kaposi's sarcoma-associated herpesvirus (KSHV), are putative etiologic agents for Burkitt lymphoma, nasopharyngeal carcinoma, and some cases of gastric cancers, and Kaposi's sarcoma, multicentric Castleman's disease, and primary effusion lymphoma (PEL) especially in AIDS setting for the latter case, respectively. Since such two viruses mentioned above are highly species specific, it has been quite difficult to prove their oncogenic activities in animal models. Nevertheless, the viral oncogenesis is epidemiologically and/or *in vitro* experimentally evident. This time, we investigated gene expression profiles of KSHV-oriented lymphoma cell lines, EBV-oriented lymphoma cell lines, and T-cell leukemia cell lines. Both KSHV and EBV cause a B-cell-originated lymphoma, but the gene expression profiles were typically classified. Furthermore, KSHV could govern gene expression profiles, although PELs are usually coinfected with KSHV and EBV.

1. Introduction

Several viruses could induce cancers in human beings. For examples, some papilloma viruses (PVs) should be etiologic agents for cervical cancers [1], hepatitis B virus (HBV) [2] and hepatitis C virus (HCV) [3] for hepatocellular carcinomas, human T-lymphotropic virus 1 (HTLV-1) for adult T-cell leukemia (ATL) [4], Epstein-Barr virus (EBV) for Burkitt lymphomas, nasopharyngeal carcinomas (NPCs), and some of gastric carcinomas [5, 6], and Kaposi's sarcoma-associated virus (KSHV) for Kaposi's sarcoma [7], primary effusion lymphomas (PELs), and multicentric Castleman's disease [8–13]. Recently, a newly identified polyomavirus, Merkel cell polyomavirus, is nominated as an etiologic agent for Merkel cell carcinoma [14]. These viruses have too narrow host ranges to meet Koch's principles, and, therefore, there are a lot of augments about it. Nevertheless, causation between the viral infection and the related cancer formation could be evident epidemiologically and *in vitro* experimentally.

Chronic inflammation caused by these viruses should be important factors, but it is not forgettable to keep in our minds that such inflammation itself is primarily caused by the viral infection [17]. Except for HCV and HTLV-1, these oncogenic viruses are usually DNA viruses and establish persistent or latent infection [18, 19]. Of course, HCV also establishes persistent infection in the infected hepatocytes [3]. Parts of some viral genomes in case of DNA viruses are integrated into host genomes, even though the process is not included in the life cycles. Integration could play roles for oncogenesis as shown for retroviral oncogenesis, and; thus, integration of viral genomes leads to promoter insertion mechanism to activate putative cellular oncogenes and host genome fragility [20]. If viral oncogenes are integrated and expressed, the effect should be more direct.

γ-herpesviruses such as EBV and KSHV are DNA viruses and do not have the genome integration process in their life cycles and just present as episomes in the infected nuclei for lives after establishing latent infection, since their genomes replicate and are partitioned according to the host cell cycles by utilizing host cellular replication machinery [6, 9]. Thus, the genomes act as complete extra genomes.

KSHV was found in Kaposi's sarcoma tissues with representational difference analysis (RDA) as the eighth human herpesvirus by Chang et al. [21]. The sequence analysis revealed that this virus is not a member of $\gamma 1$ or lymphocryptoviruses, which includes EBV, but $\gamma 2$ or rhadinoviruses, whose prototype is Herpesvirus saimiri [22]. Extensive studies about the relationship between the virus infection and the diseases have shown that this virus is a causative agent for Kaposi's sarcoma [7], primary effusion lymphomas (PELs), and multicentric Castleman's disease [8], most of which happen in acquired immunodeficiency syndrome setting [23]. As for KS, KSHV is usually present in all types of KS: classical, iatrogenic, and African endemic KS and human immunodeficiency virus-1 negative gay men with KS [24]. Thus, it is doubtless that KSHV is an etiologic agent for KS and two lymphoproliferative diseases such as PEL and MCD as various kinds of γ-herpesviruses are related to some cancer formation [19].

KSHV has two life cycles: lytic infection/reactivation and latent infection as known for all herpesviruses. Among eight human herpesviruses, only EBV and KSHV establish latency *in vitro* especially Burkitt lymphoma [25] cell lines and PEL cell lines, respectively. In the latency, the viruses express a limited number of genes and replicate according to host cell cycle. The replicated genomes are partitioned into daughter cells, and; thus, the same copy number of the viral episomes is maintained, though details of the mechanism remain to be elucidated [26].

In case of KSHV, the viral latency seems to be very important for the maintenance of PEL, since the loss of the viral episomes leads to PEL cell death. Furthermore, EBV and KSHV usually coinfected in PEL but EBV is frequently lost while establishing PEL cell lines [27]. It has been unable for us to find out or establish subclones of KSHV-negative PEL cell lines from the parental lines [28]. In contrast, an EBV-lost BL cell line has been established [29].

Recently, we investigated gene expression profiles of several PEL cell lines [30] TY1 [31], BCBL1 [32], and its derivative D90 [28], BC3 [27], BC1 [33], in order to know the characteristic gene expression to maintain the PEL cells, comparing with those of BL lines: Ramos, Daudi, BJAB, Raji, and Akata [34]. And including T-cell-originated lymphoma cell lines: Jurkat, Molt3, SupT1 and MT4, we tried to know common features leading to lymphoma formation. Among PEL cell lines, only BC1 is coinfected with KSHV and EBV. BL cell lines are usually infected with EBV except Ramos and BJAB in the lineups this time. MT4 contains integrated human T-cell leukemia virus 1 (HTLV-1) genomes. Typically, the gene expression profiles were classified into either B-cell-originated or T-cell-originated pattern. And KSHV-associated PEL and usually EBV-associated BL showed typical gene expression profiles, respectively. Even though there was only one PEL cell line infected both with KSHV and EBV, its gene expression profile was classified as a KSHV pattern, suggesting that KSHV might make stronger influence on gene expression in the infected cells. In this paper, we would like to discuss and review about gene expression profiles of KSHV-associated B-cell lymphoma or lymphoma-like disease, while mining new data from our DNA array analysis or comparing ours to the others.

2. Gene Expression Profiles of KSHV-Related Tumors

As mentioned above, there are three definite diseases caused by KSHV. They are KS, PEL, and MCD. Especially in AIDS setting, KSHV has a very tight link with these diseases, and that is the virulence of KSHV emerges under the condition. It seems to be meaningful to know gene expression profiles of tumors, since such gives us information about origin of tumor cells, mechanism of tumorigenesis, designs of treatment, and so on. And thus; several reports have been published [25].

2.1. Kaposi's Sarcoma. The cellular origin of the spindle cells of KS is poorly defined and could be originated from vascular endothelial cells and various kinds of cytokines, chemokines, and growth factors are expressed [35, 36]. A recent report has shown that KSHV reprograms transcription profiles from angiogenic to lymphatic ones by inducing *PROX1*, a master regulator of lymphatic development and downregulation of blood vascular genes, in infected human dermal microvascular endothelial cells (HDMECs) [37, 38]. KSHV induces LYVE-1, reelin, follistatin, and desmoplakin as well as *PROX1*. These findings suggest that KSHV infection should induce a comprehensive reprogramming of blood vascular endothelial cells (BECs) to adopt a lymphatic endothelial cells (LECs). In the tissues of KS, a kind of cytokine and interleukin-6 (IL-6), basic fibroblast growth factor (bFGF), tumor necrosis factor-α (TNF-α), oncostatin M, interferon-γ (IFN-γ), and so on storm happens. In *in vitro* KSHV infection study; however, IL-6, oncostatin M, TNF-α, and IFN-γ inductions were not induced. In contrast, tumor growth factor $\beta 1/\beta 3$ and TGFb R2, CCL5 [39], CCL8 (MCP-2) and CCR5, and angiopoietin-2 (ang-2) were induced. Though such differences might be dependent on differences from environment for preparation of samples, some factors could be synthesized and secreted from the other kinds of cell type, because KS is actually a mixture of various kinds of tissues [35]. KS is basically latently infected with KSHV, and, thus usually does not express KSHV lytic genes [40]. It is, however, possible that lytic cycle is turned on especially just upon the infection and some lytic genes such as viral IL-6 (vIL-6), viral chemokines (vMIP-I, vMIP-II, and vMIP-III), possible oncogenic genes, such as K1, viral G-protein-coupled receptor (vGPCR) are expressed transiently and make an effect on various kinds of cellular gene expression [37]. Though details about mechanism remain to be understood, replication and transcription activator (RTA), a viral immediate early gene and a key inducer of viral lytic replication, must be expressed for lytic replication cycle. RTA is an extremely strong transactivator and functions both in a sequence-specific and a nonspecific manner. RTA could induce critical cellular gene expression and make a direction to KS formation [41, 42].

2.2. Multicentric Castleman's Disease. KSHV causes two B-cell-originated lymphoproliferative diseases: MCD and PEL [16]. MCD is a polyclonal and a kind of reactive lymphoproliferative disorder characterized by KSHV-infected monotypic cytoplasmic IgM-λ-expressing plasmablasts residing primarily in the mantle zone, dissolution of the follicles, and prominent interfollicular vascular proliferation [7]. MCD cells resemble mature B cells, as they express the preplasma cell markers, IRF4 and BLIMP1, the memory B-cell marker CD27, OCT2, and Ki67, though they are negative for certain B-cell-associated marker such as Pax5, CD20, CD30, and CD138 (syndecan-1) [43]. MCD plasmablasts are reported not to show somatic hypermutation in their rearranged IgV genes [7]. KSHV might preferentially target IgM-λ-expressing native B cells and differentiate into plasmablasts bypassing the GC reaction, although not all MCDs are infected with KSHV. In MCD, EBV is rarely coinfected [44]. It seems quite an interesting story, since both of viruses can infect a B-cell lineage and EBV usually disseminates more than 90% human beings and probably preexist in B cells before KSHV enters. It is unclear and should be elucidated whether MCD does not emerge in the presence of EBV, or development of MCD excludes EBV from the cells.

It has not been successful to observe lymphoproliferation *in vitro* by infecting KSHV with peripheral blood mononuclear cells as shown for EBV, though KSHV infects $CD19^+B$ cells and establishes latency therein [32, 45]. From a point of view of gene expression profiles, high level interleukin 6 (IL-6) expression is a well-known fact in MCD and should do something in MCD pathogenesis [46]. B-cell markers, CD20 and the memory B-cell marker CD27 are usually expressed, but B-cell activation markers such as CD23, CD38 and CD30 are not [43]. KSHV gene expression profiles are different from those in KS and PEL. It was reported that viral lytic genes, vIRF-1 and vIL-6, and ORF59 (a polymerase processivity factor, PF8) as well as a latent gene, LANA, were expressed, suggesting that not a few cells in MCD are in the lytic phase [47].

2.3. Primary Effusion Lymphoma (PEL). PEL is a distinct subtype of non-Hodgkin's lymphoma associated with KSHV as mentioned. PEL most commonly presents with pleural, peritoneal, or pericardial malignant effusions without a contiguous tumor mass [16]. In contrast to MCD, PEL is usually coinfected with EBV in vivo, and; therefore, EBV could be involved in the onset of tumor formation. It could be likely that PEL with or without EBV is different from origin of B-cell differentiation state [48]. KSHV, however, is never lost when PEL is introduced into cell culture maintenance *in vitro*, even if EBV frequently is lost from PEL cell lines. Thus, there is a strong linkage between the existence of KSHV and the maintenance of PEL cell lines *in vitro*. PEL is thought to be originated from post-GC plasmablastic cells [49]. Both PEL and MCD have a plasmablastic phenotype but should be different in the terms whether they are post-GC or bypass-GC reaction, respectively, [50].

EBV is another human oncogenic γ-herpesvirus, a putative causative agent of BL, NPC, some gastric carcinoma, NK lymphoma, and so on [6]. BL is also originated from GC B-cell and known for *MYC-IgH* or *MYC-IgL* rearrangement [15, 51]. Study on gene expression profiles using *in vitro* infection systems showed that cyclin-dependent kinase inhibitor 1 (CDKN1A; CIP1/WAF1; p21, U09579), interleukin-15 receptor α subunit precursor (U31628), interferon-induced 56-kd protein (IFI-56 K, X31628), and protein-tyrosine phosphatase 1C (PTP1C) SHP1 (X62055) and HLA class II histocompatibility antigen α chain (K01171) and HLA-DR antigen-associated invariant subunit (X00497) were prominently induced by the factor of ten or more [52]. High-mobility group protein (HMG-I, M23619), proliferating cyclic nuclear antigen (PCNA, M15796), endonuclease III homolog I (U79718), poly(ADP-ribose) polymerase (PARP; PPOL, M18112), erythroblastosis virus oncogene homolog1 (ETS-1, J04101), p-GAP hematopoietic protein C1 (RGC1, X78817), and c-myc (V00568) were remarkably reduced by the factor of five to eight hundred [52]. In this paper, EBV was infected with EBV-negative BL cell lines. The infected cells showed latency III phenotype, which is corresponding to lymphoblastoid cell lines (LCLs) established by EBV infection to PBMC *in vitro*. Most of BL, however, show latency I phenotype, and thus; this experiment model reflects LCL rather than BL [6]. Another report also utilized an EBV-depleted BL cell line, EBV^- Akata [53]. EBV^- Akata and EBV^+ Akata were stimulated with IgG crosslinking, and lytic replication was induced. They analyzed cellular gene expression as well as viral gene expression. In this case, data did not reflect effects of EBV on BL, since this was just lytic replication/reactivation process, and almost all viral genes were expressed, which presumably took a substantial effect on cellular gene expression.

We recently investigated gene expression profiles of PEL cell lines, comparing with those of the other uniquely categorized cell lines, one of which was BL cell lines with or without EBV infection and another of which was T-cell leukemia cell lines (TCLs) [30]. All PEL cell lines are infected with KSHV, and one of them, BC1, is coinfected with KSHV and EBV. BL cell lines are usually infected with EBV, but Ramos and BJAB are not infected with EBV. TCL cell lines are heterogeneous. Jurkat was established from an acute T-cell leukemia, and Molt-3 and SupT1 were from a respective T-lymphoblastic leukemia, and MT4 was from an adult T-cell leukemia. Thus, differentiation status may be different among lines.

Our obtained results were that three kinds of lines were typically classified into respective groups. Although the results might reflect just differentiation status of these cell lines, KSHV would never be lost from the PEL cell lines and BC1 coinfected with KSHV, and EBV was classified into the PEL cell category, suggesting that KSHV should be more dominant in gene expression control. Among about thirty thousand genes analyzed this time, we could extract sixty-three genes typically higher in BL cell lines and also sixty genes predominantly higher in PEL cell lines. For example, CD79A (NM_001738) and B (NM_000626), which are components of B-cell receptor and contain cytoplasmic immunoreceptor tyrosine-based

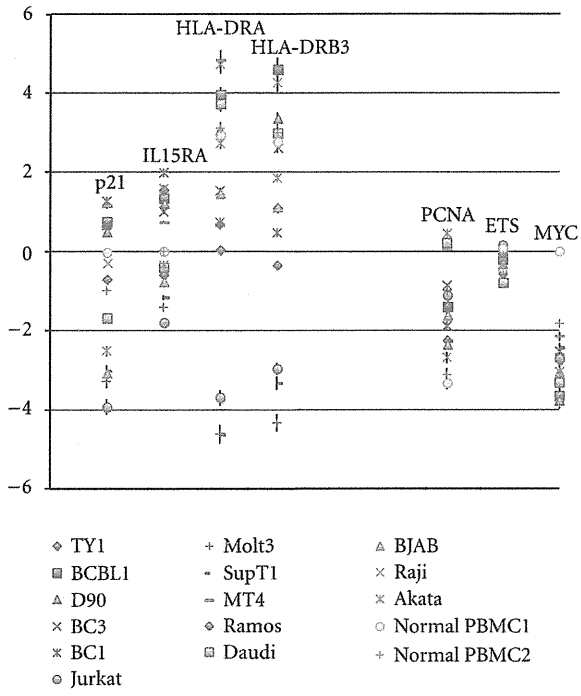

FIGURE 1: Genes increased or decreased in the presence of EBV [15] are picked up. The increased genes; $p21^{Cip1/WAF1}$, IL15RA, HLA-DRA, and HLA-DRB3 were checked. The decreased genes: PCNA, ETS, and MYC (represented as N-myc in our case) were checked. Data are shown as $\log_2$ values with standard deviation. The concrete mean value of each gene expression was shown in Table 1.

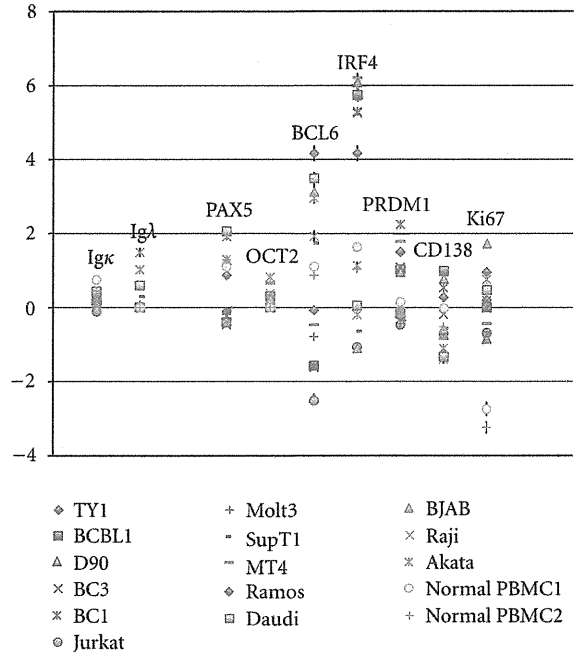

FIGURE 2: Genes characteristic in MCD are picked up. In MCD, Igκ, PAX5, BCL6, CD138 are usually not expressed [16]. On the other hand, Igλ, OCT2, IFR4/MUM1, PRDM1/BLINP1, and Ki67 are expressed [16]. Data are shown as $\log_2$ values with standard deviation. Characterization among PEL, BL, and TCL is shown in Table 2.

Table 1

Name	ID	TY1	BCBL1	D90	BC3	BC1	Jurkat	Molt3	SupT1	MT4	Ramos	Daudi	BJAB	Raji	Akata	Normal PBMC1	Normal PBMC2
p21, Cip1 (CDKN1A), transcript variant 1	NM-000389	0.6168	0.7342	0.4951	0.6498	1.2574	−3.9304	−3.2876	−3.0266	1.1385	−0.7121	−1.6921	−3.071	−0.2815	−2.5181	−0.0306	−0.9993
IL15RA transcript variant 1	NM-002189	1.5549	1.3211	1.2054	1.0005	1.9795	−1.7987	−1.4156	−1.1644	0.7295	−0.6013	−0.4221	−0.7741	1.5869	−0.3408	0	0
HLA-DRA	NM-019111	0.6808	3.9458	3.0478	1.5288	0.7271	−3.696	−4.6163	−4.6238	4.8328	0.0282	3.7191	1.4575	4.7263	2.7318	2.9285	3.1007
HLA-DRB3	AF192259	1.1026	4.5938	3.344	2.6277	0.4602	−2.9625	−4.33	−3.3242	4.657	−0.3435	2.9802	1.1189	4.2563	1.8549	2.7688	2.9922
PCNA, transcript variant 1	NM-002592	−2.2538	−1.4012	−2.3533	−0.8696	−1.8885	−1.111	−1.0025	−2.2581	0.0462	−1.3735	0.2045	−1.6252	−2.6854	0.4512	−3.3202	−3.1112
ETS oncogenes	L16464	−0.2124	−0.2223	−0.1314	−0.6449	−0.6913	0.1483	−0.1052	0.0186	−0.0974	−0.0638	−0.8105	−0.3384	−0.3456	−0.5868	0.0757	−0.1052
MYCN	NM-005378	−2.7601	−3.6677	−3.7899	−2.5286	−2.7087	−2.7141	−3.2058	−2.4416	−2.1501	−3.3287	−3.329	−3.0585	−3.7126	−3.0375	0	−1.8303

Table 2

Lines	Gene						
	IRF4/MUM1	PRDM1/BLINP1	CD138	PAX5	BCL6	OCT2	Ki67
PEL	↑↑	↑	↑	↓	↓	→	→
BL	↑	→	↓	↑	↑↑	→	→
TCL	↓	↓	↓	↓	↓	→	↓

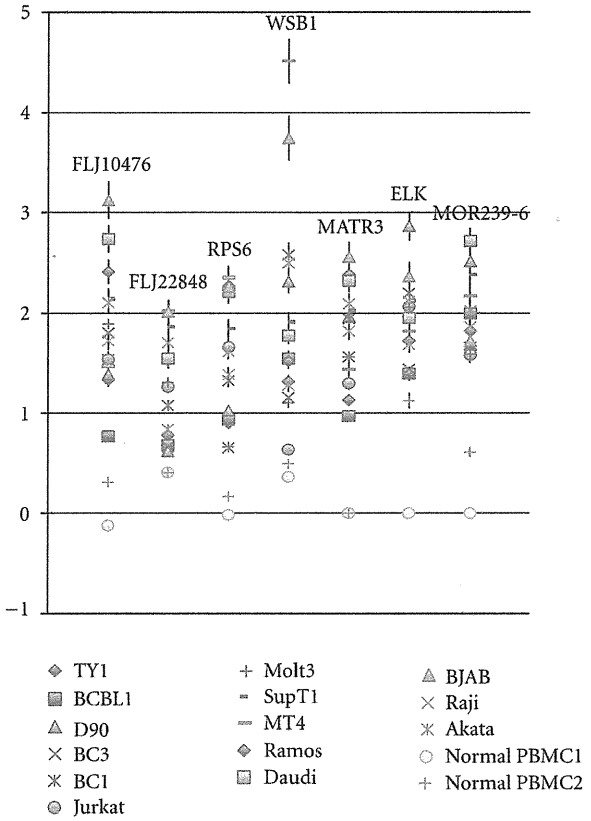

Figure 3: Highly expressing genes all in PEL, BL, and TCL are picked up. Data are shown as $\log_2$ values with standard deviation. Data are shown as $\log_2$ values with standard deviation. Detailed mean value of each gene is shown in Table 3.

activation motifs were highly expressed in BL without doubt. Accordingly, BCR downstream signaling 1 (BRDG1, NM_012108) was also higher in BL cell lines. A mature B cell-marker, CD22 (NM_001771), was characteristically expressed in BL not in PEL. Among very highly expressing genes in PEL, we found methyl CpG-binding domain protein (MBD1, NM_015845), interleukin 2 receptor beta (IL2RB, NM_000878), and angiopoietin 1 (ANGPT1, NM_001146). Such gene expression in PEL might suggest cellular environment and pathophysiologic status in the patient bodies under immunosuppression due to AIDS established by human immunodeficiency virus 1 (HIV-1) and KSHV infection.

Focused on $p21^{Cip1/WAF1}$ (NM_000389), IL15 receptor α (NM_002189) and HLA-DR (HLA-DRA, NM_019111; HLA-DRB3, AF192259), which are reported to increase by EBV infection, this gene expression was indeed higher in B cell originated PEL and BL with a few exceptions in our analysis (Figure 1, Table 1). PCNA, ETS (L16464), and MYC (NM_005378) were relatively higher in TCL again with several exceptions, though MYC-Ig rearrangement was a feature of BL.

Paying attention to genes characteristic to MCD, a naïve B-cell marker: surface Ig lambda (XM_066332), B-cell specific markers: PAX 5 (NM_016734), Oct2 (XM_068123), and a GC B-cell marker: BCL6 (NM_001706) were higher in BL cell lines and preplasma cell markers; IRF4/MUM1 (NM_002460) and PRDM1/BLIMP1 (NM_001198) are definitely higher in PEL cells, assuring that BL should be derived from GC B cell and PEL from post-GC plasmablasts (Figure 2, Table 2). Plasma cell marker, CD138 (NM_002997), was also higher in PEL. Memory B-cell markers, Oct2 and Ki67 (NM_002417) expression, were not so different among three types of cell lines. Collectively, decisive differences between PEL and BL are low CD138 in

TABLE 3

Name	ID	TY1	BCBL1	D90	BC3	BC1	Jurkat	Molt3	SupT1	MT4	Ramos	Daudi	BJAB	Raji	Akata	Normal PBMC1	Normal PBMC2
cDNA FLJ10476	AK001338	1.3263	0.7676	1.3801	1.7984	1.5367	1.5343	1.882	2.1362	1.4682	2.4062	2.7347	3.1228	1.7163	2.098	−0.1203	0.3065
cDNA: FLJ22848	AK026501	0.7782	0.6786	0.6153	0.6563	1.0736	1.2594	1.3044	1.8615	2.0176	1.5196	1.5458	2.0081	1.7023	0.8386	0.4045	0.4004
Ribosomal protein S6 (RPS6)	NM_001010	0.9017	0.9334	1.0244	0.6479	1.3239	1.6572	0.6572	1.8411	2.3493	2.2682	2.1999	2.2522	1.3873	1.6164	−0.0182	0.1647
WD repeat and SOCS box-containing 1 (WSB1), transcript variant 1	NM_015626	1.3127	1.5445	2.3089	1.1516	2.5711	0.6377	1.0981	1.9078	4.5103	1.5161	1.7749	3.7406	1.2755	2.4918	0.359	0.4896
Matrin 3 (MATR3)	NM_018834	1.1246	0.968	1.9522	1.5564	1.9376	1.2933	1.5574	2.0226	1.4332	2.3825	2.3212	2.5539	1.8178	2.0884	0	0
ELK (LOC131341)	XM_067332	1.7184	1.391	2.8614	1.4346	2.1936	2.0576	2.0501	2.1184	1.813	1.9541	1.9471	2.3651	2.1104	1.6868	0	1.121
Similar to olfactory receptor MOR239-6	XM_372502	1.6318	1.9947	2.5101	1.6554	2.706	1.5783	1.5849	2.3774	2.1667	1.8178	2.711	1.7203	1.8556	2.0178	0	0.603

TABLE 4

Name	ID	TY1	BCBL1	D90	BC3	BC1	Jurkat	Molt3	SupT1	MT4	Ramos	Daudi	BJAB	Raji	Akata	Normal PBMC1	Normal PBMC2
cDNA FLJ20118	AK000125	−2.3823	−1.9072	−1.9797	−1.8911	−2.6889	0	−2.1411	−3.2798	−2.5236	−2.1555	−2.0963	−2.7591	−1.9995	−3.0018	0	0
cDNA FLJ12884	AK022946	−2.8453	−2.4261	0	−2.737	−2.4877	−2.3244	−0.8999	−1.0235	−1.4208	−2.4356	−3.054	−3.0835	−2.7217	−2.5435	0	0
cDNA FLJ13038	AK023100	−2.9994	−2.4772	−3.0186	−3.3026	−2.7287	−3.3596	−0.9996	−0.183	−2.7834	−2.658	−2.4415	−2.4291	−2.2883	−2.1052	0.3132	0.1399
cDNA FLJ13209	AK023271	−2.9254	−3.6178	−3.8287	−3.3465	−2.8999	−2.3812	−4.33	−2.8324	−3.6977	−3.658	−3.481	−3.5892	−3.4616	−3.7744	0	−0.5065
cDNA FLJ14567	AK027473	−3.3823	−3.6178	−2.7058	−1.8379	−3.0182	−1.3668	−2.0374	−2.2945	−1.1757	−3.073	−2.6242	−3.8415	−3.3297	−2.4208	0	−1.7585
cDNA FLJ31353	AK055915	−3.5001	−4.7198	−4.1118	−3.7967	−3.6791	−2.7417	−3.8866	−2.9092	−4.0524	−3.0009	−2.66	−2.2996	−1.3509	−4.1115	−0.3823	−0.1246
cDNA FLJ37955	AK095274	−1.2998	−0.1113	−1.5633	−1.317	−0.7984	−2.5666	−1.8192	−1.5649	−0.9224	−1.412	−2.5134	−2.0463	−2.5324	−1.4445	0	0
Odz3	AK125869	−2.0213	−2.4624	−1.4756	−1.3957	0	−2.9199	−2.5731	0	−2.6255	−2.2639	−2.4891	−2.0586	−2.4616	−2.5606	0	−1.0642
COL1A2	NM_000089_(2)	−3.44	−3.3222	−4.0878	−4.1915	−2.749	−3.696	−3.9297	0	−3.7933	−3.1489	−3.2724	−3.3744	−3.2883	−3.7349	0	0
Cystatin C (CST3)	NM_000099	−2.4327	−4.907	−6.1118	−1.2356	−5.4965	−2.5502	−3.4042	−3.4663	−1.4284	−5.6953	−6.1657	−2.9177	−5.7681	−5.5523	0.8547	1.1031
HBG2	NM_000184	−3.0213	−3.5694	−5.6968	−4.589	−3.1337	−4.9735	−5.8868	−4.6997	−5.983	−4.989	−5.0186	−4.4372	−6.0162	−5.7744	2.1347	0.3396
LYZ	NM_000239	−5.6627	−5.492	−6.0191	−3.9692	−5.5666	−6.0181	−5.1158	−5.3856	−5.3393	−5.8556	−4.8031	−4.7591	−5.3724	−4.9903	3.8701	4.0167
Serine (or cysteine) proteinase inhibitor	NM_000295	−5.2996	−1.4884	−4.5925	−5.7768	−5.245	−5.9302	−6.0676	−5.5169	−5.8128	−5.4198	−5.973	−5.8415	−5.7681	−5.5523	−1.0957	−1.0244
Interleukin 8 (IL8)	NM_000584	−3.066	−2.2442	−1.7518	−3.2322	−2.2886	−1.9093	−1.5561	−2.3167	−1.0642	−0.786	−2.1655	−2.3976	−1.9719	−0.8359	0.2761	1.0034
Interleukin 8 (IL8)	NM_000584_(2)	−4.5312	−3.1113	−3.6435	−2.4952	−3.6218	−3.7141	−3.7453	−2.7393	−2.7447	−4.3286	−4.4183	−2.8521	−3.5085	−3.4525	0.6967	1.5545
ANXA1	NM_000700	−1.6884	−2.7462	−5.7704	−4.139	−2.1007	−5.5584	−1.2667	−0.7569	−1.2654	−5.1886	−5.8851	−5.7587	−5.6238	−5.3593	−0.1914	−0.0244
TNFRSF1B	NM_001066	−0.0646	0.4257	−0.2587	1.098	0.1654	0.2687	0.0731	0.1623	0.208	−0.3584	−0.6991	0.0238	0.6067	−0.1162	2.0232	2.1586
ANPEP	NM_001150	−2.4773	−1.7507	−2.6092	−2.7866	−2.7593	−3.0066	−3.0552	−2.458	−2.3106	−1.6907	−2.3004	−2.5452	−2.1459	−2.0679	0.5172	0.5893
APOC1	NM_001645	−3.6284	−3.538	−2.7898	−3.554	−3.8226	−3.9735	−4.6522	−3.2088	−3.1376	−3.814	−4.0902	−3.9982	−3.6943	−4.0374	0	0
CRYAB	NM_001885	−1.994	−2.3767	−2.7519	−2.8275	−1.1204	−1.4943	−2.7645	−1.347	−1.245	−1.2816	−2.2518	−1.4818	−2.3089	−1.4287	0	0
GZMK	NM_002104	−3.7509	−1.7642	−3.2504	−2.8275	−3.0557	−3.9954	−3.6702	−3.6613	−2.8032	−2.2499	−3.3004	−2.2636	−2.2547	−2.2233	0.5673	0.6936
JUN	NM_002228	−2.2409	−2.7734	−3.1238	−0.3842	−1.8718	−0.968	−0.4387	−0.1644	−0.0479	−0.1719	−4.1148	−2.9517	−2.454	−3.7744	1.5962	0.4284
CD73 (NT5E)	NM_002526	−3.5469	−3.5694	−2.9525	−2.1262	−4.3968	−2.9955	−3.0552	−3.4173	−3.0405	−4.162	−3.53	−2.5027	−3.4164	−3.0495	0	0

Table 4: Continued.

Name	ID	TY1	BCBL1	D90	BC3	BC1	Jurkat	Molt3	SupT1	MT4	Ramos	Daudi	BJAB	Raji	Akata	Normal PBMC1	Normal PBMC2
PLAU	NM_002658	−1.32	−1.3256	−1.0046	−1.9922	0	−1.7095	−2.8448	0	0	−1.564	−2.6154	−2.3216	−2.005	−2.4366	0	0
CCL4	NM_002984	−4.0775	−3.0884	−3.2772	−3.6609	−3.8663	−4.0179	−4.2461	−3.7799	−3.2966	−3.8773	−3.1025	−3.0341	−0.0679	−2.7947	−0.2159	0.5398
ADAM12	NM_003474	−3.2734	−2.4118	−2.4872	−3.9021	−3.1744	−2.7141	−2.8448	−4.1018	−1.7494	−1.4316	−2.245	−2.8415	−2.3438	−1.2267	0	0
CST7	NM_003650	−4.8452	−3.9896	−4.0644	−4.9018	−4.4624	−2.9199	−2.9627	−3.2088	−3.7163	−3.0126	−3.7061	−3.8629	−3.59	−3.1371	−0.4389	−0.3123
Transmembrane protein with EGF-like	NM_003692_(2)	−2.671	−2.4047	0	−2.7765	−2.8225	−0.806	−1.1992	−1.3585	−2.3392	−2.3888	−2.642	−2.2147	0.3012	−2.8359	0	0
SEMA5A	NM_003966	−2.8649	−1.8483	0	−2.4386	−2.8885	−2.9304	−3.0552	−2.5429	−1.7116	−0.949	−2.1785	−2.5281	−1.9556	−1.4326	0	0
GNG11	NM_004126	−4.0104	−3.4189	−4.3748	−3.2049	−4.0558	−3.696	−3.9517	−4.0512	−3.2966	−4.0608	−3.9956	−2.2285	−3.0276	−3.535	0.048	0.2964
GZMB	NM_004131	−2.8163	−2.7373	−3.1483	−2.4788	−2.5577	−2.6085	−2.9627	−3.141	−2.1376	−2.5947	−3.4031	−3.0585	−2.8869	−2.5097	−0.3744	0.161
CSPG2	NM_004385	−2.8949	−2.3492	−3.3043	−2.6702	−3.2887	−3.3739	−3.4663	−3.6804	−1.2017	−3.0009	−3.4493	−2.8846	−2.8665	−3.4849	2.5309	2.5699
DUSP1	NM_004417	−2.0379	−0.9817	−1.9471	−1.6749	−1.8718	−1.5061	−0.9489	−1.1083	−0.0928	−0.8586	−2.0841	−0.4291	−1.1583	−1.8891	3.5758	3.3222
HRG-gamma	NM_004495	−3.0435	−2.7642	−3.5591	−3.3918	−3.365	−3.0066	−3.6702	−3.2088	−2.5484	−2.8349	−3.1273	−2.8415	−3.5733	−2.6315	0	0
PARG1	NM_004815	−3.579	−2.8197	−3.3321	−3.4545	−3.6218	−2.678	−2.6794	−3.0388	−3.2966	−2.0305	−3.9068	−3.4694	−3.1961	−2.4445	−1.0763	0
MYCN	NM_005378	−2.7601	−3.6677	−3.7899	−2.5286	−2.7087	−2.7141	−3.2058	−2.4416	−2.1501	−3.3287	−3.329	−3.0585	−3.7126	−3.0375	0	−1.8303
S100A11	NM_005620	−0.7903	−1.5457	−0.8165	−0.6245	−3.1072	−6.1108	−3.2326	−1.5212	−0.8772	−4.9434	−5.8851	−4.0462	−5.5571	−5.0866	−0.621	−0.388
S100A12	NM_005621	−1.8649	−2.5536	−2.3462	−3.3918	−2.2447	−1.863	−2.6611	−3.1148	−1.8131	−1.5468	−2.0481	−2.8415	−2.4389	−1.9388	3.5746	3.8939
SH3BP4	NM_014521	−2.0548	−2.5457	−2.7802	−3.2185	−1.8551	−2.374	−2.9853	−2.6997	−2.8641	−2.6396	−3.1149	−2.7391	−2.5244	−2.7546	0	0
SAMHD1	NM_015474	−1.7555	−2.2633	−2.2307	−2.1326	−2.3417	−3.9735	−4.2737	−3.4173	−2.4362	−1.7002	0.468	−2.6528	−1.6283	−0.3059	1.9357	2.0445
RAI14	NM_015577	−3.1478	−3.5225	−3.1857	−3.1135	−2.6889	0	−3.9079	−2.8007	−1.417	−1.3361	−2.9729	−3.5367	−2.7684	−3.9443	0	0
SH2D4A	NM_022071	−2.0049	−0.9299	−0.4187	−2.8589	−1.6987	−2.111	−2.3374	−1.8217	−1.4284	−0.7936	−1.9068	−2.0161	−1.4771	−1.5014	0	0
MATN2, transcript variant 2	NM_030583	−1.8949	−2.8873	−2.4563	−2.5976	−2.531	−3.1598	−2.5561	−2.2653	−2.4517	−2.2923	−3.1528	−2.5195	−2.4616	−3.4849	0	0
PTPNS1	NM_080792	−2.8748	−1.5575	−3.6787	−2.5118	−2.9697	−1.5791	−2.4194	−2.0954	−1.8081	−2.4922	−2.66	−2.0834	−2.4771	−2.0926	0.6197	0.1952
Similar to TCR delta chain (LOC122700)	XM_058650	−3.1358	−2.0828	−3.0413	−3.2459	−3.0684	−2.9199	−2.7452	−2.9903	−2.3832	−0.412	−2.803	−2.6161	−2.3368	−0.9728	1.3643	1.7152

PEL and high in BL, very low BCL6 in PEL, and very high in BL (Figure 2, Table 2). In addition, very strong expression of IRF4/MUM1 in PEL was characteristic, compared to the other cell lines.

If there are common genes in all tumor cell lines analyzed this time, such genes could be generally required for their establishment and/or maintenance. Thus, we mined the data in such point of view and found a couple of genes were commonly overexpressed compared to normal PBMC (Figure 3, Table 3). It is interesting that these include genes involved in signaling. However, since most of genes are not known well for their function, it remains to be clarified what they do and how important they are.

In the same way, we also mined the data to find less expression in all types of cell line (Table 4), which might give disadvantage to cancer formation and/or maintenance. Actually, we found fifty or so of such genes, most of them are functionally unknown, and detailed analyses will be required in near future (data not shown).

3. Conclusions

Studying gene expression profiles gives us various kinds of information. The analysis especially in cancer will lead to understanding how cancers are generated and maintained and to design what to do in order to suppress cancer growth. It is, however, just screening, and we have much work to do for this aim.

References

[1] P. M. Howly and D. R. Lowy, *Papillomaviruses*, Lippincott Williams & Wilkins, Philadelphia, Pa, USA, 2007.

[2] D. Kremsdorf, P. Soussan, P. Paterlini-Brechot, and C. Brechot, "Hepatitis B virus-related hepatocellular carcinoma: paradigms for viral-related human carcinogenesis," *Oncogene*, vol. 25, no. 27, pp. 3823–3833, 2006.

[3] M. Levrero, "Viral hepatitis and liver cancer: the case of hepatitis C," *Oncogene*, vol. 25, no. 27, pp. 3834–3847, 2006.

[4] M. Matsuoka and K. T. Jeang, "Human T-cell leukaemia virus type 1 (HTLV-1) infectivity and cellular transformation," *Nature Reviews Cancer*, vol. 7, no. 4, pp. 270–280, 2007.

[5] L. S. Young and A. B. Rickinson, "Epstein-Barr virus: 40 years on," *Nature Reviews Cancer*, vol. 4, no. 10, pp. 757–768, 2004.

[6] A. B. Rickinson and E. Kieff, *Epstein-Barr Virus*, Lippincott Williams & Wilkins, Philadelphia, Pa, USA, 2007.

[7] M. Q. Du, H. Liu, T. C. Diss et al., "Kaposi sarcoma-associated herpesvirus infects monotypic (IgMλ) but polyclonal naive B cells in Castleman disease and associated lymphoproliferative disorders," *Blood*, vol. 97, no. 7, pp. 2130–2136, 2001.

[8] D. P. McDonagh, J. Liu, M. J. Gaffey, L. J. Layfield, N. Azumi, and S. T. Traweek, "Detection of Kaposi's sarcoma-associated herpesvirus-like DNA sequences in angiosarcoma," *American Journal of Pathology*, vol. 149, no. 4, pp. 1363–1368, 1996.

[9] D. Ganem, *Kaposi's Sarcoma-Associated Herpesvirus*, Lippincott Williams & Wilkins, Philadelphia, Pa, USA, 2007.

[10] U. R. Hengge, T. Ruzicka, S. K. Tyring et al., "Update on Kaposi's sarcoma and other HHV8 associated diseases. Part 2: pathogenesis, Castleman's disease, and pleural effusion lymphoma," *Lancet Infectious Diseases*, vol. 2, no. 6, pp. 344–352, 2002.

[11] U. R. Hengge, T. Ruzicka, S. K. Tyring et al., "Update on Kaposi's sarcoma and other HHV8 associated diseases. Part 1: epidemiology, environmental predispositions, clinical manifestations, and therapy," *Lancet Infectious Diseases*, vol. 2, no. 5, pp. 281–292, 2002.

[12] P. S. Moore and Y. Chang, "Kaposi's sarcoma-associated herpesvirus immunoevasion and tumorigenesis: two sides of the same coin?" *Annual Review of Microbiology*, vol. 57, pp. 609–639, 2003.

[13] R. Sarid, S. J. Olsen, and P. S. Moore, "Kaposi's sarcoma-associated herpesvirus: epidemiology, virology, and molecular biology," *Advances in Virus Research*, vol. 52, pp. 139–232, 1999.

[14] H. Feng, M. Shuda, Y. Chang, and P. S. Moore, "Clonal integration of a polyomavirus in human Merkel cell carcinoma," *Science*, vol. 319, no. 5866, pp. 1096–1100, 2008.

[15] R. Dalla Favera, S. Martinotti, and R. C. Gallo, "Translocation and rearrangements of the c-myc oncogene locus in human undifferentiated B-cell lymphomas," *Science*, vol. 219, no. 4587, pp. 963–967, 1983.

[16] E. Cesarman and D. M. Knowles, "The role of Kaposi's sarcoma-associated herpesvirus (KSHV/HHV-8) in lymphoproliferative diseases," *Seminars in Cancer Biology*, vol. 9, no. 3, pp. 165–174, 1999.

[17] S. I. Grivennikov, F. R. Greten, and M. Karin, "Immunity, inflammation, and cancer," *Cell*, vol. 140, no. 6, pp. 883–899, 2010.

[18] D. Elgui de Oliveira, "DNA viruses in human cancer: an integrated overview on fundamental mechanisms of viral carcinogenesis," *Cancer Letters*, vol. 247, no. 2, pp. 182–196, 2007.

[19] B. Damania, "Oncogenic γ-herpesviruses: comparison of viral proteins involved in tumorigenesis," *Nature Reviews Microbiology*, vol. 2, no. 8, pp. 656–668, 2004.

[20] H. Varmus, "Retroviruses," *Science*, vol. 240, no. 4858, pp. 1427–1435, 1988.

[21] Y. Chang, E. Cesarman, M. S. Pessin et al., "Identification of herpesvirus-like DNA sequences in AIDS-associated Kaposi's sarcoma," *Science*, vol. 266, no. 5192, pp. 1865–1869, 1994.

[22] J. J. Russo, R. A. Bohenzky, M. C. Chien et al., "Nucleotide sequence of the Kaposi sarcoma-associated herpesvirus (HHV8)," *Proceedings of the National Academy of Sciences of the United States of America*, vol. 93, no. 25, pp. 14862–14867, 1996.

[23] A. Potthoff, N. H. Brockmeyer, M. Stucker, U. Wieland, A. Kreuter, and H. A. Competence Network, "Kaposi sarcoma in a HIV uninfected man who has sex with men," *European Journal of Medical Research*, vol. 15, no. 2, pp. 79–80, 2010.

[24] C. Boshoff and R. A. Weiss, "Kaposi's sarcoma-associated herpesvirus," *Advances in Cancer Research*, vol. 75, pp. 57–86, 1998.

[25] P. P. Naranatt, H. H. Krishnan, S. R. Svojanovsky, C. Bloomer, S. Mathur, and B. Chandran, "Host gene induction and transcriptional reprogramming in kaposi's sarcoma-associated herpesvirus (KSHV/HHV-8)-infected endothelial, fibroblast, and B cells: insights into modulation events early during infection," *Cancer Research*, vol. 64, no. 1, pp. 72–84, 2004.

[26] K. Ueda, S. Sakakibara, E. Ohsaki, and K. Yada, "Lack of a mechanism for faithful partition and maintenance of the KSHV genome," *Virus Research*, vol. 122, no. 1-2, pp. 85–94, 2006.

[27] L. Arvanitakis, E. A. Mesri, R. G. Nador et al., "Establishment and characterization of a primary effusion (body cavity-based) lymphoma cell line (BC-3) harboring Kaposi's sarcoma-associated herpesvirus (KSHV/HHV-8) in the absence of Epstein-Barr virus," *Blood*, vol. 88, no. 7, pp. 2648–2654, 1996.

[28] K. Nishimura, K. Ueda, S. Sakakibara et al., "Functional analysis of Kaposi's sarcoma-associated herpesvirus RTA in an RTA-depressed cell line," *Journal of Human Virology*, vol. 4, no. 6, pp. 296–305, 2001.

[29] N. Shimizu, A. Tanabe-Tochikura, Y. Kuroiwa, and K. Takada, "Isolation of Epstein-Barr virus (EBV)-negative cell clones from the EBV- positive Burkitt's lymphoma (BL) line Akata: malignant phenotypes of BL cells are dependent on EBV," *Journal of Virology*, vol. 68, no. 9, pp. 6069–6073, 1994.

[30] K. Ueda, E. Ito, M. Karayama, E. Ohsaki, K. Nakano, and S. Watanabe, "KSHV-infected PEL cell lines exhibit a distinct gene expression profile," *Biochemical and Biophysical Research Communications*, vol. 394, no. 3, pp. 482–487, 2010.

[31] H. Katano, Y. Hoshino, Y. Morishita et al., "Establishing and characterizing a CD30-positive cell line harboring HHV-8 from a primary effusion lymphoma," *Journal of Medical Virology*, vol. 58, no. 4, pp. 394–401, 1999.

[32] R. Renne, W. Zhong, B. Herndier et al., "Lytic growth of Kaposi's sarcoma-associated herpesvirus (human herpesvirus 8) in culture," *Nature Medicine*, vol. 2, no. 3, pp. 342–346, 1996.

[33] E. Cesarman, P. S. Moore, P. H. Rao, G. Inghirami, D. M. Knowles, and Y. Chang, "In vitro establishment and characterization of two acquired immunodeficiency syndrome-related lymphoma cell lines (BC-1 and BC-2) containing Kaposi's sarcoma-associated herpesvirus-like (KSHV) DNA sequences," *Blood*, vol. 86, no. 7, pp. 2708–2714, 1995.

[34] K. Takada, K. Horinuchi, Y. Ono et al., "An Epstein-Barr virus-producer line Akata: establishment of the cell line and analysis of viral DNA," *Virus Genes*, vol. 5, no. 2, pp. 147–156, 1991.

[35] B. Herndier and D. Ganem, "The biology of Kaposi's sarcoma," *Cancer Treatment and Research*, vol. 104, pp. 89–126, 2001.

[36] S. A. Miles, "Kaposi sarcoma: a cytokine-responsive neoplasia?" *Cancer Treatment and Research*, vol. 63, pp. 129–140, 1992.

[37] H. W. Wang, M. W. B. Trotter, D. Lagos et al., "Kaposi sarcoma herpesvirus-induced cellular reprogramming contributes to the lymphatic endothelial gene expression in Kaposi sarcoma," *Nature Genetics*, vol. 36, no. 7, pp. 687–693, 2004.

[38] Y. K. Hong, K. Foreman, J. W. Shin et al., "Lymphatic reprogramming of blood vascular endothelium by Kaposi sarcoma-associated herpesvirus," *Nature Genetics*, vol. 36, no. 7, pp. 683–685, 2004.

[39] M. Weinreb, P. J. Day, F. Niggli et al., "The role of Epstein-Barr virus in Hodgkin's disease from different geographical areas," *Archives of Disease in Childhood*, vol. 74, no. 1, pp. 27–31, 1996.

[40] L. L. Decker, P. Shankar, G. Khan et al., "The Kaposi sarcoma-associated herpesvirus (KSHV) is present as an intact latent genome in KS tissue but replicates in the peripheral blood mononuclear cells of KS patients," *Journal of Experimental Medicine*, vol. 184, no. 1, pp. 283–288, 1996.

[41] J. Chen, K. Ueda, S. Sakakibara, T. Okuno, and K. Yamanishi, "Transcriptional regulation of the Kaposi's sarcoma-associated herpesvirus viral interferon regulatory factor gene," *Journal of Virology*, vol. 74, no. 18, pp. 8623–8634, 2000.

[42] K. Yada, E. Do, S. Sakakibara et al., "KSHV RTA induces a transcriptional repressor, HEY1 that represses rta promoter," *Biochemical and Biophysical Research Communications*, vol. 345, no. 1, pp. 410–418, 2006.

[43] A. Chadburn, E. M. Hyjek, W. Tam et al., "Immunophenotypic analysis of the Kaposi sarcoma herpesvirus (KSHV; HHV-8)-infected B cells in HIV+ multicentric Castleman disease (MCD)," *Histopathology*, vol. 53, no. 5, pp. 513–524, 2008.

[44] E. Oksenhendler, M. Duarte, J. Soulier et al., "Multicentric Castleman's disease in HIV infection: a clinical and pathological study of 20 patients," *Aids*, vol. 10, no. 1, pp. 61–67, 1996.

[45] D. Dittmer, C. Stoddart, R. Renne et al., "Experimental transmission of kaposi's sarcoma-associated herpesvirus (KSHV/HHV-8) to SCID-hu Thy/Liv mice," *Journal of Experimental Medicine*, vol. 190, no. 12, pp. 1857–1868, 1999.

[46] T. S. Uldrick, V. Wang, D. O'Mahony et al., "An interleukin-6-related systemic inflammatory syndrome in patients co-infected with kaposi sarcoma-associated herpesvirus and HIV but without multicentric castleman disease," *Clinical Infectious Diseases*, vol. 51, no. 3, pp. 350–358, 2010.

[47] C. Parravicini, B. Chandran, M. Corbellino et al., "Differential viral protein expression in Kaposi's sarcoma-associated herpesvirus-infected diseases: Kaposi's sarcoma, primary effusion lymphoma, and multicentric Castleman's disease," *American Journal of Pathology*, vol. 156, no. 3, pp. 743–749, 2000.

[48] R. Hamoudi, T. C. Diss, E. Oksenhendler et al., "Distinct cellular origins of primary effusion lymphoma with and without EBV infection," *Leukemia Research*, vol. 28, no. 4, pp. 333–338, 2004.

[49] A. Matolcsy, R. G. Nador, E. Cesarman, and D. M. Knowles, "Immunoglobulin V(H) gene mutational analysis suggests that primary effusion lymphomas derive from different stages of B cell maturation," *American Journal of Pathology*, vol. 153, no. 5, pp. 1609–1614, 1998.

[50] R. Kuppers, "Mechanisms of B-cell lymphoma pathogenesis," *Nature Reviews Cancer*, vol. 5, no. 4, pp. 251–262, 2005.

[51] R. Taub, I. Kirsch, and C. Morton, "Translocation of the c-myc gene into the immunoglobulin heavy chain locus in human Burkitt lymphoma and murine plasmacytoma cells," *Proceedings of the National Academy of Sciences of the United States of America*, vol. 79, no. 24, pp. 7837–7841, 1982.

[52] F. Baran-Marszak, R. Fagard, B. Girard et al., "Gene array identification of Epstein Barr virus-regulated cellular genes in EBV-converted Burkitt lymphoma cell lines," *Laboratory Investigation*, vol. 82, no. 11, pp. 1463–1479, 2002.

[53] J. Yuan, E. Cahir-McFarland, B. Zhao, and E. Kieff, "Virus and cell RNAs expressed during Epstein-Barr virus replication," *Journal of Virology*, vol. 80, no. 5, pp. 2548–2565, 2006.

5

Kaposi's Sarcoma-Associated Virus Governs Gene Expression Profiles Toward B Cell Transformation

Keiji Ueda[1], Emi Ito[2], Masato Karayama[3], Eriko Ohsaki[1], Kazushi Nakano[1] and Shinya Watanabe[2]
[1]*Division of Virology, Department of Microbiology and Immunology Osaka University Graduate School of Medicine*
[2]*Department of Clinical Genomics, Translational Research Center Fukushima Medical University*
[3]*Department of Infectious Diseases, Hamamatsu University School of Medicine Japan*

1. Introduction

Kaposi's sarcoma-associated herpesvirus (KSHV), also called human herpesvirus-8 (HHV-8) was found in patients' specimens as a causative agent of Kaposi's sarcoma by representational difference analysis (RDA) (Chang et al., 1994). Initially identified fragments by RDA were KS330Bam and KS631Bam, which showed a sequence similarity to a portion of the open reading frame (ORF) 26 open reading frame encoding the capsid protein VP23 of herpesvirus saimiri (HVS) and the amino acid sequence encoded by the corresponding BDLF1 ORF of Epstein-Barr virus (EBV), and to the tegment protein, ORF75 and also the tegment protein of EBV, BNRF1 (p140), respectively. The following full sequence analysis revealed that KSHV was belonging to the γ-herpesvirus subfamily, the genus rhadinovirus rather than lymphocryptic virus and could be a new oncogenic DNA virus (Moore et al., 1996; Russo et al., 1996).

KSHV is supposed to infect various kinds of tissue *in vitro* at least by using integrin αVβ3 as a receptor (Garrigues et al., 2008) and establishes latency in B cells (Chen and Lagunoff, 2005). KSHV has been reported to infect a primary endothelial cell and can transform it into a spindle cell which is a characteristic feature of the oncogenic activity of KSHV in endothelial cells (Lagunoff et al., 2002) However, it has not been revealed effective *in vitro* infection to primary peripheral blood mononuclear cells (PBMC), which of course include B cell, as EBV can form lymphoblastoid cell lines (LCL). Extensive studies so far have revealed that KSHV should be an etiologic agent for Kaposi's sarcoma (KS), multicentric Castleman's disease (MCD), and primary effusion lymphoma (PEL) (Hengge et al., 2002a; Hengge et al., 2002b).

It is quite a big question how oncogenic viruses are involved in their related cancers. Especially limited host ranges of viruses only infecting with humans make this question more unanswerable. One approach to get a hint about this question and solve it is to see gene expression profiles of viruses-associated tumors. Recently, we analyzed three types of typical lymphocyte-originated tumor cell lines-primary effusion lymphoma (PEL) cell lines,

T cell leukemia cell lines (TCL), Burkitt lymphoma (BL) cell lines-and two sets of PBMCs-in order to know how PEL was generated by searching characteristic gene expression profiles. Our approach, however, might be just to show typical gene expression profiles after establishment of PEL cell lines and it may be very difficult to account for viral pathogenesis only by gene expression profiles. Needless to say, we need an experimental model to observe the whole process from virus infection to cancer formation. In this chapter, we discuss about how KSHV is involved in PEL formation and what to do next to solve questions about viral oncogenesis.

2. Characteristic features of KSHV

KSHV is a γ-herpesvirus mentioned above and the genome is double stranded linearized DNA about 170kb long including GC-rich repetitious repeat called terminal sequences (TR), the unit of which is 801bp and repeated 30~50 times at the end of the genome though the sequence and the repeated unit might be different among clones. The unique region of the genome is about 140kb long and encodes more than 80 genes, most of which are lytic genes (Russo et al., 1996). The linearized genome is circularized at the TR after entry into cells and usually stealthies as an episome not going to full lytic replication.

2.1 KSHV life cycles

Like the other herpesviruses, KSHV has two typical life cycles called lytic infection (or reactivation from latency) and latent infection. Lytic infection/reactivation is a virus producing cycle and probably all viral genes are expressed from immediate early (IE), early (E) and late (L) genes in a cascade-like fashion. A key factor for lytic replication is Reactivation Transcription Activator (RTA) (Chen et al., 2001; Lukac et al., 1998; Sun et al., 1998). RTA is a very strong transactivator and trans-activates the other viral E genes such as *K-bZIP* (*K8*), *orf57*, *pan* including *kaposin* (*k12*), a latent gene, not only through specific binding sequences but also through an indirect mechanism (Sakakibara et al., 2001). When L genes are successfully expressed, it leads to explosive daughter virus production, which is a final end of the viral life cycle to disseminate viral infection and survive as its virus itself in nature.

On the other hand, latent infection is a viral stealthing state. The viral genome replicates according to the host cell cycle and is partitioned into divided cells at least in KSHV infected PEL cell lines (Ballestas, Chatis, and Kaye, 1999). The viral copy number per cell appears to be maintained at the same (Ueda et al., 2006). In this state, expressing viral genes are extremely limited to a few genes such latency-associated nuclear antigen (*lana*), viral cyclin (*v-cyc*), viral flip (*v-flip*), kaposin (*k12*) and viral interferon regulatory factor 3 (*v-irf-3*) (Paulose-Murphy et al., 2001). The former three genes are actually in one unit of gene (Fig. 1). *lana* and *v-cyc-v-flip* expression is regulated by alternative splicing. *v-cyc-v-flip* is in one transcript and v-FLIP is translated through internal ribosome entry site (IRES). Although *k12* is an independent gene, these four genes are present in one region and actively expressed. It remains to be solved how latent genes are regulated, since neighbor genes just upstream or downstream are tightly inactivated in a high density of genes in the genome. Epigenetic marking might be important to establish this state but it is unclear how such an effect itself is controlled (Toth et al., 2010). As for a virus, latency is a kind of poised state waiting for lytic replication, because it could be unfavorable for the virus to disseminate and expand its generation.

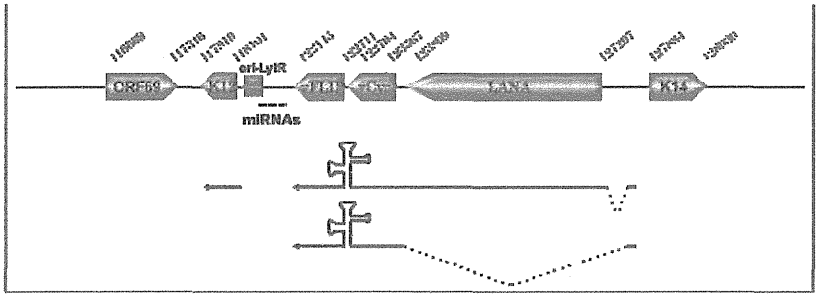

Fig. 1. The active gene locus around *lana*.

The viral latency might be the places for KSHV-associated malignancies mentioned below, since such malignancies usually show viral latent infection. And therefore, it seems to be quite important to understand what the viral latency is and it will give us hints to investigate functions of the viral latent genes products. Nevertheless, if the viral latenct genes products work for cellular immortalization and/or transformation, there may be more patients in KSHV infected people suffering from KSHV-associated malignancies. Thus, it should be kept in our mind to take this idea into consideration when thinking how KSHV is involved in cancer formation.

2.2 Latency-associated nuclear antigen (LANA)

LANA is one of the most actively produced viral factors and controls the viral latency. Though LANA seems to be a multifunctional protein, important functions of LANA in the latency are to support the viral genome replication, to partition the replicated viral genome and to maintain the same genome copy number per cell, and to regulate the viral genes expression (Han et al., 2010).

LANA has two binding sites called LANA binding sequences (LBS) in TR and replication origin of the KSHV genome in latency (ori-P) consists of the LBS and the following 32bp GC-rich segment (32GC) (Garber, Hu, and Renne, 2002; Garber et al., 2001). One of two LBS is required for the viral replication at least but it is not enough, i.e., 32GC is also required (Hu and Renne, 2005). Though it remains to be solved how the viral ori-P is determined among repeated TR sequences and how 32GC is functioning, LANA has been reported to interact with components of cellular replication machinery; origin recognition complex 1 to 6 (ORC1~ORC6) (Verma et al., 2006). Probably LANA binds with LBS and recruits ORCs on the ori-P to start replication. It is, however, very questionable whether LANA binds all ORCs at the same time. LANA also interacts with a histone acetyltransferase binding to ORC1 (HBO1) and epigenetic control around ori-P is may be more important (Stedman et al., 2004).

LANA is supposed to interact with a chromosome component, since the viral genomes are found in the vicinity of chromosomes and actually reported to bind with a histone such as H2B, and with Bub1, CENP-F and so on (Barbera et al., 2006; Xiao et al., 2010). Such interaction might account for the viral genome partition and maintenance, though the detail is unclear.

LANA regulates the viral genes expression and maybe cellular gene expression by interacting with components involved in heterochromatin formation such as heterochromatin protein 1 (HP1) and histone methyl transferase, suv39H1. LANA binds with LBS and recruits such

factors on the viral genome, which forms heterochromatin-like environment of the genome and as a whole inactive gene expression (Sakakibara et al., 2004).
Viral genes expressed in the latency might have oncogenic activities because KSHV-associated malignancies are usually in latency setting. Multifunctional LANA interacts with many cellular factors other than those mentioned above. Several mechanisms are thought how LANA works in the viral oncogenesis. LANA interacts with suppressive oncogenes such as p53 (Friborg et al., 1999) as the other oncogenic DNA viral genes products. We have confirmed that LANA interacts with p53 to degradade (Suzuki et al., 2010) but not pRb (our personal observation). It was also reported that LANA interacted with glycogen synthase kinase 3β (GSK3β) and blocked β-catenin degradation pathway that was promoted β-catenin phosphorylation by GSK3β (Liu et al., 2007). On the other hand, stably LANA expressing cells are, however, very difficult to establish, which means that LANA expression might give disadvantage for cell growth rather than cell growth promotion (our personal observation).

2.3 Viral cyclin (v-CYC)

KSHV encodes a cyclin D homologue termed v-cyclin, which is translated from alternatively spliced mRNA covering the *lana-v-cyc-v-flip* region (Li et al., 1997) (Fig. 1). v-CYC interacts with cyclin dependent kinase 6 (CDK6) and promotes G1-S progression (Godden-Kent et al., 1997; Swanton et al., 1997). The Cyclin D-CDK6 complex is to function to exit from G0 to G1 phase (Laman et al., 2001) and the v-cyc/CDK6 complex is resistant to inhibition by CDK inhibitors by p16, p21 and p27 (Jarviluoma et al., 2004). Thus, its real function has not been elucidated and it was reported that ectopic or overexpression of c-CYC evokes rather cell/DNA damage (Koopal et al., 2007).

2.4 Viral FLICE inhibitory protein (v-FLIP)

KSHV encoded *v-flip*, a homologue of cellular flip (*c-flip*) is expressed as co-transcript with *v-cyc* and translated via internal ribosome entry site (IRES). v-FLIP activates NF-kB to maintain PEL cell tumor phenotype (Guasparri, Keller, and Cesarman, 2004). Inhibition of NF-kB activity and knocking down v-FLIP lead to KSHV infected PEL cell death (Keller, Schattner, and Cesarman, 2000). NF-kB activity is also required for maintenance of KSHV latency (Ye et al., 2008) and v-FLIP, thus, may sustain the viral latency in B cells to stand by for oncogenic transformation and maintain the transformed phenotype (de Oliveira, Ballon, and Cesarman, 2010). Oncogenic activity of v-FLIP was also reported and in transgenic mice models, v-FLIP expression induces B cell transdifferentiation and tumorigenesis (Ballon et al., 2011). Furthermore, v-FLIP represses cell death with autophagy by interacting Atg3 (Lee et al., 2009).

2.5 Kaposin (K12)

Kaposin is a uniquely transcribed at the edge of the active transcription region of the KSHV genome (Li et al., 2002). There are three frames around this region and probably a major gene is so-called *kaposin B* whose C-terminal region is corresponding to K12 ORF. Open reading frame (ORF) of KAPOSIN B contains reiterated proline-rich, 23-amino acid direct repeats, since this region includes one of two ori-Lyt sequences (lytic replication origin) (Sadler et al., 1999). KAPOSIN B activates p38 mediated mitogen-activated protein kinase [MAPK]-associated protein kinase 2 (MK2) make AU-rich 3′ UTR containing mRNA stabilize (McCormick and Ganem, 2005). Activation of p38, on the other hand, was reported